Bifunctional Chelates Optimized for Molecular MRI

Erik C. Wiener,[†] Marie-Caline Abadjian,[‡] Raghvendra Sengar,[†] Luce Vander Elst,[§] Christoffel Van Niekerk,[‡] Douglas B. Grotjahn,*[,‡] Po Yee Leung,[‡] Christie Schulte,[‡] Curtis E. Moore,[⊥] and Arnold L. Rheingold[⊥]

[†]Hillman Cancer Center, University of Pittsburgh Medical Center, 5117 Centre Avenue, Pittsburgh, Pennsylvania 15213, United States

[‡]Department of Chemistry and Biochemistry, San Diego State University, 5500 Campanile Drive, San Diego, California 92182-1030, United States

[§]Department of General, Organic and Biomedical Chemistry, University of Mons, 7000 Mons, Hainaut, Belgium

[⊥]Department of Chemistry and Biochemistry, University of California, San Diego, La Jolla, California 92093-0385, United States

Ⓢ Supporting Information

ABSTRACT: Important requirements for exogenous dyes or contrast agents in magnetic resonance imaging (MRI) include an effective concentration of paramagnetic or superparamagnetic ions at the target to be imaged. We report the concise synthesis and characterization of several new enantiopure bifunctional derivatives of $(\alpha^1R,\alpha^4R,\alpha^7R,\alpha^{10}R)$-$\alpha^1,\alpha^4,\alpha^7,\alpha^{10}$-tetramethyl-1,4,7,10-tetraazacyclododecane-1,4,7,10-tetraacetic acid (DOTMA) (and their 1,4,7,10-tetraazacyclododecane-1,4,7,10-tetraacetic acid (DOTA) analogues as controls) that

can be covalently attached to a contrast agent delivery system using either click or peptide coupling chemistry. Gd complexes of these derivatives can be attached to delivery systems while maintaining optimal water residence time for increased molecular imaging sensitivity. Long chain biotin (LC-biotin) derivatives of the Eu(III) and Gd(III) chelates associated with avidin are used to demonstrate higher efficiencies. Variable-temperature relaxometry, ^{17}O NMR, and nuclear magnetic resonance dispersion (NMRD) spectroscopy used on the complexes and biotin−avidin adducts measure the influence of water residence time and rotational correlation time on constrained and unconstrained systems. The Gd(III)-DOTMA derivative has a shorter water residence time than the Gd(III)-DOTA derivative. Compared to the constrained Gd(III)-DOTA derivatives, the rotationally constrained Gd(III)-DOTMA derivative has ~40% higher relaxivity at 37 °C, which could increase its sensitivity as an MRI agent as well as reduce the dose of the targeting agent.
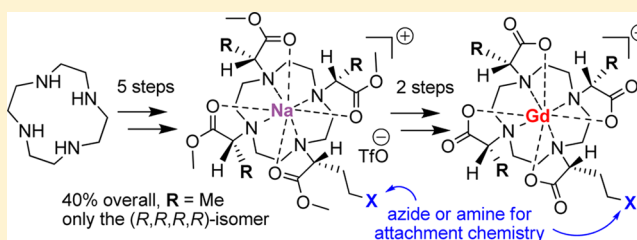
The enormous versatility of magnetic resonance imaging (MRI) offers the promise of combining anatomical images with noninvasive in vivo histopathology, molecular and cellular imaging, imaging metabolic pathways, and functional imaging. Over the years MRI has achieved a number of successes, including dynamic contrast enhancement (DCE) MRI[1,2] as a marker of changing vascular endothelial growth factor[3,4] in cancer, imaging receptor expression,[5−11] stem cell tracking,[12−16] transporter systems,[17−20] using choline[21−23] as a marker for the PI3K pathway,[24−26] the use of intracellular sodium[27,28] for imaging cell division,[29] and blood oxygen level monitoring.[30−33] No matter the MR technique, one either needs to use exogenous markers or endogenous markers.

The use of exogenous dyes or contrast agents requires a suitable concentration of the agent at the desired target. To achieve detection, a number of approaches have been used including delivery of relatively large numbers of paramagnetic or superparamagnetic ions (such as Gd, Mn, and Fe) in the form of polymeric drug delivery systems[34,35] and/or nanoparticles,[6,8−10] or a smaller number of more highly efficient agents, or a combination of the two.[7,36,37]

Free, unchelated gadolinium is generally toxic; hence, sequestering it as a kinetically stable chelate is vital to reduce toxicity to acceptable levels. A synthetic challenge addressed in this work is the creation of a bifunctional chelating system that has all of the following favorable properties: (1) rapid water exchange that allows highly efficient relaxation and increased sensitivity, (2) tight Gd^{3+} binding, and (3) easy covalent attachment to a desired structure while maintaining the properties that allow highly efficient relaxation and increased sensitivity.

The sensitivity of any method described above depends on the efficiency of the agent (relaxivity) either at the level of the individual ion or the entire molecule. Relaxivity is calculated as the change in relaxation rate ($1/T_1$ or $1/T_2$) per unit concentration of ion. Higher relaxivities result in more efficient contrast agents and lower doses or an increased ability to detect low-expression targets. The most common form of magnetic
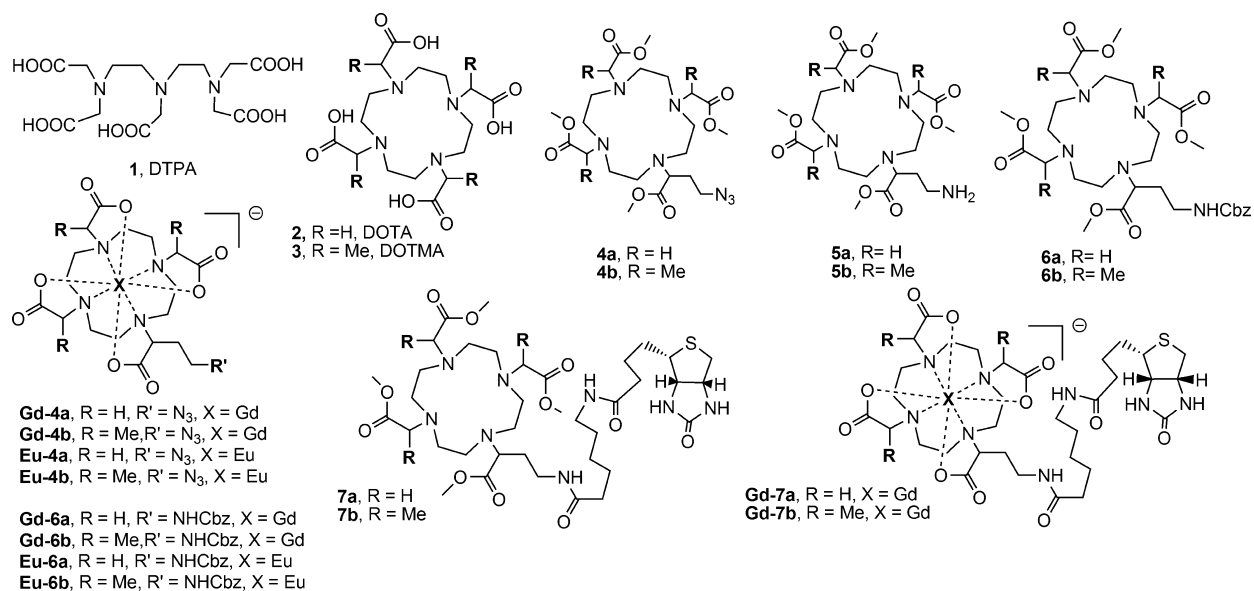
Figure 1. Known (**1**−**3**) chelators for Gd and novel bifunctional compounds (**4**−**7**) made in this study.

resonance imaging (MRI) contrast agent works through dipole−dipole interactions of the paramagnetic ion with water protons. The chemist can alter variables in three categories (inner-,[38−41] second-,[42] and outer-sphere[43,44] contributions) to optimize efficiency of a contrast agent. The inner-sphere contribution depends on the number of water molecules directly coordinated to the metal ion (q), the time that the water molecules remain coordinated to the ion (the water residence time, τ_M), the number of unpaired electrons (or spin quantum number, S), the distance between the metal ion dipole and dipole of the interest (r), the electronic relaxation time (τ_S), and a measure of rotational diffusion or the rotational correlation time (τ_R). The second-sphere contribution depends on similar variables, which are associated with the second coordination sphere. The outer-sphere contribution depends on the number of unpaired electrons or spin quantum number (S), the electronic relaxation time (τ_S), the distance between the metal ion dipole and dipole of the interest (d), and the relative diffusion coefficient D such that d^2/D is the translational correlation time (τ_D). For T_1-based agents with long electronic relaxation times, such as gadolinium [Gd(III)] in the 0.2 to 3.0 T range commonly used in the clinic, the best method to increase the efficiency of an agent is to increase the rotational correlation time (τ_R).

Attaching ion-chelate complexes to macromolecules increases the rotational correlation time and the relaxivity.[36,37,41,45] Initial studies conjugated monofunctional chelates to macromolecules by linking one of the chelate carboxylic acids to an amine on the macromolecule to form an amide bond. This resulted in an increase in relaxivity that was significantly less than expected.[41] Using variable-temperature relaxivity studies Lauffer et al.[41] predicted that the water residence time was so long that it limited the relaxivity gains associated with increasing the rotational correlation time. Using the same method, others[46] confirmed in general that Gd(III) chelates containing amide ligands had water residence times long enough to negate relaxivity gains associated with increasing the rotational correlation time. At about the same time by direct measurement of the water−oxygen exchange rate, Gonzalez et al.[47] confirmed a long water residence time for

the bismethyl−amide derivative of diethylenetriamine pentaacetic acid (DTPA) (**1**, Figure 1) complexed to Gd(III) (2325 ns at 25 °C). They also reported that the water residence times of both Gd(III)-DTPA and Gd(III)-DOTA are long, 244 and 208 ns, respectively (DOTA = 1,4,7,10-tetraazacyclododecane-1,4,7,10-tetraacetic acid).

Theoretical studies predict that the optimum water residence time for maximizing the relaxivity by increasing the rotational correlation time of Gd(III)-based agents is between 10 to 60 ns.[41,48] The direct measurements of the water residence time of Gd complexes with either DTPA[49] or DOTA[49] (**1** or **2**, Figure 1) or their amide[47] derivatives mentioned above confirmed that the water residence times are greater than 200 ns. When coupled with variable-temperature relaxometry studies, direct measurements confirm that the water residence time of Gd(III)-DOTA and Gd(III)-DTPA limits the gains in relaxivity associated with increasing the rotational correlation time.[48,50−53]

For the DOTA chelate two conformational isomers are present, each with different water residence times and relaxivity properties. It is well-known that modifications in the structure of DOTA or its analogues such as adding a methyl group to each acetate arm (to yield ($\alpha^1 R,\alpha^4 R,\alpha^7 R,\alpha^{10}R$)-$\alpha^1,\alpha^4,\alpha^7,\alpha^{10}$-tetramethyl-1,4,7,10-tetraazacyclododecane-1,4,7,10-tetraacetic acid (DOTMA)) so that the complex is homochiral (Gd-R,R,R,R-DOTMA, **3**) or fusing cyclohexyl rings to the backbone results in faster water exchange rates or shorter water residence times and higher relaxivities of rotationally constrained systems. The higher relaxivities result from shifting the relative population of isomers to the one(s) with faster water exchange.[54−57]
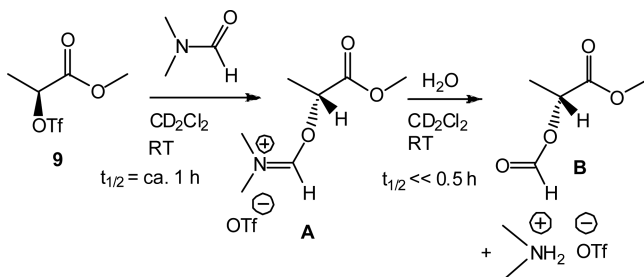
The discussion above indicates that contrast agents prepared from Gd(III)-DOTMA should be more efficient and have higher relaxivities than those prepared from Gd(III)-DOTA, but the problem until the work reported here is that the existing strategy for covalent attachment of the macrocycle−use of one carboxylate for amide formation−leads to longer water residence times and reduced relaxivities. Therefore, to leave the tetracarboxylate ligand system intact, we designed and prepared new bifunctional derivatives of DOTA and DOTMA

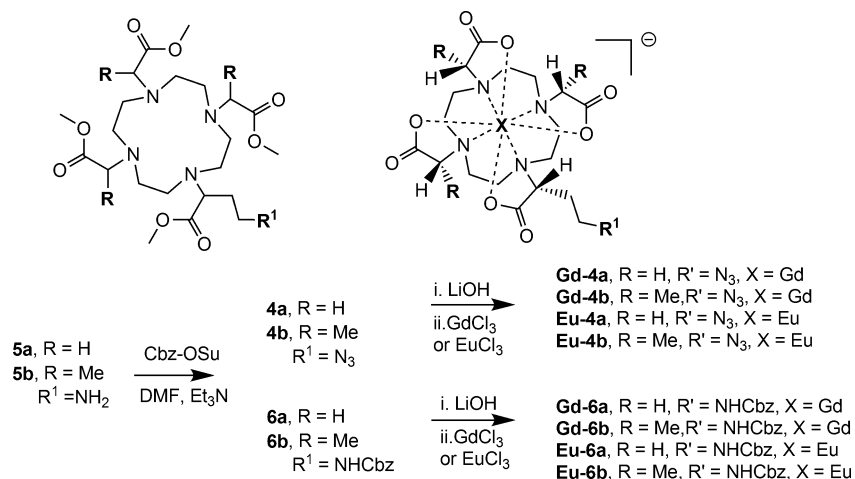**Scheme 1. Synthesis of 4b-NaOTf and Amine Analogue 5b-NaOTf**
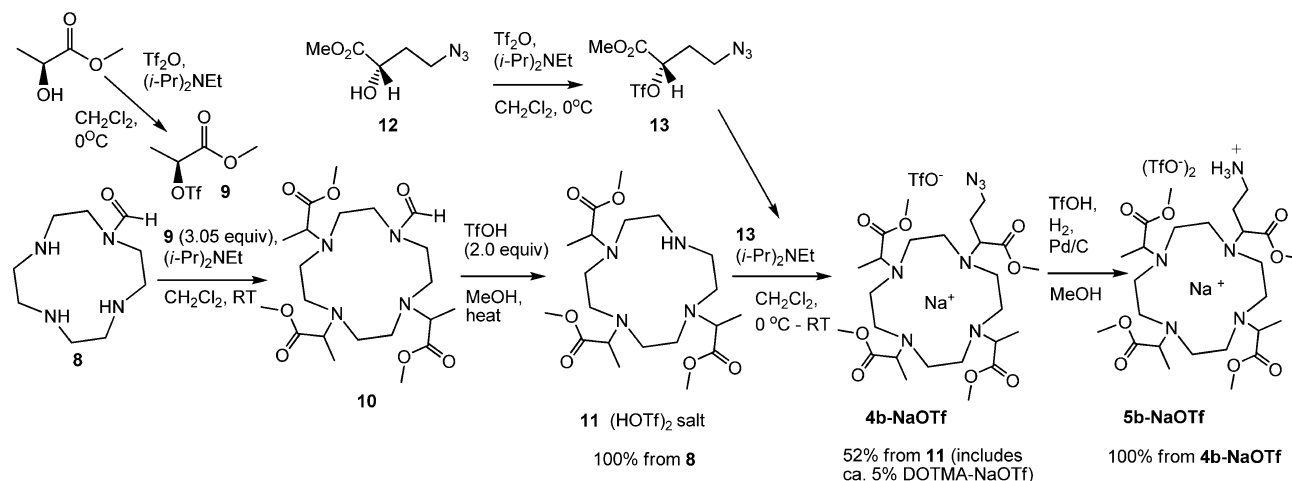
(Figure 1), either bearing an azide-bearing side chain (**4a** and **4b**, respectively) that can be linked to alkynes using click chemistry[58] (not shown in this work) or bearing an amine (**5a** and **5b**, respectively) for linking to carboxylic acids using standard peptide ligation methods, as shown in Scheme 1. Once coordinated to Gd or Eu, the resulting bifunctional agents would be novel, versatile complexes that could selectively react through click chemistry or peptide coupling, depending on the need, to conjugate the chelate to a molecule of interest (see Scheme 2). In contrast, commercially available bifunctional imaging agents typically use carboxylate-active ester or isothiocyanate groups for covalent attachment, unfortunately compromising one or more of the chelating carboxylate arm(s) and disrupting the optimal coordination geometry favored by homochiral DOTMA; thus, they are not as effective. In this report we describe the synthesis of **4a,b** and **5a,b** and the derivatization of **5a,b** with either a Cbz group or biotinylated chain. Chelates for the low molecular weight rapidly rotating models were derivatized at the amino group to demonstrate bifunctionality and to prevent the free amine from wrapping around and coordinating to the Gd(III), Scheme 3.

Complexation of the various new bifunctional DOTA and DOTMA species to Gd(III) allowed us to determine water residence time and relaxivity measurements of low molecular weight and macromolecular complexes of the amine derivatives. The optimal water residence time varies as a function of field strength. The complexes based on the DOTMA framework of **5** have optimal water residence times and significantly higher relaxivities (more than 50%) when rotationally constrained by biotin−avidin binding than the corresponding Gd-DOTA derivative. These higher relaxivities are expected to translate to lower doses or to the ability to detect targets at lower expression levels.

Scheme 2. Model Reactions Showing Feasibility of Deprotection of N-Formyl Group by 9 and Water

Scheme 3. Synthesis of N₃ and Cbz Model Complexes M-4a, M-4b, M-6a, and M-6b (M = Eu, Gd)

■ EXPERIMENTAL SECTION

General. Unless specified, all the reactions were done in oven-dried or flame-dried glassware in an atmosphere of dry argon gas using standard Schlenk techniques. The anhydrous solvents were purchased from Acros and Aldrich chemical companies and used in the reactions without further purification. All workup and chromatographic purifications of compounds were done in air using Optima grade solvents obtained from Fisher Scientific. Column chromatography was done using a Teledyne ISCO CombiFlash Rf automated system. Commercial grade preloaded Redi Sep Rf columns were used for silica chromatography, and HiTrap SP HP columns purchased from GE Healthcare were used for ion-exchange chromatography. The stains used to visualize the thin-layer chromatography (TLC) plates (aluminum backed 200 μm silica) were Hanessian's Stain [CeSO$_4$ (5 g) and (NH$_4$)Mo$_7$O$_{24}$.4H$_2$O (25 g) dissolved in water (450 mL) and concentrated sulfuric acid (50 mL)], and potassium permanganate stain [KMnO$_4$ (1.5 g) and K$_2$CO$_3$ (10 g) dissolved in 10% NaOH (1.25 mL) in water (200 mL)].

Caution! Although we did not observe any unusual decompositions of the azides reported, organic azides can be explosive materials and should be handled with care.

^{1}H, ^{13}C, ^{23}Na, and ^{19}F NMR spectra were recorded using Bruker ACP-500 or Varian spectrometers at 30 °C or room temperature. ^{1}H, ^{13}C, and ^{19}F NMR chemical shifts are reported in ppm referenced to residual solvent resonances (^{1}H NMR: δ 7.27 for C*H*Cl$_3$ in CDCl$_3$, and 3.31 for C*H*D$_2$OD in CD$_3$OD. ^{13}C NMR: δ 77.23 for CDCl$_3$ and 49.15 for CD$_3$OD. ^{19}F NMR: −76.55 for CF$_3$COOH). Deuterated solvents for NMR were obtained from Cambridge Isotope Laboratories and were used without purification. Electrospray ionization mass spectra (ESI MS) were collected on a Micromass Quattro II, triple quadrupole mass spectrometer using both negative and positive ionization modes. Elemental analyses were performed at NuMega Resonance Laboratories, San Diego, California. Liquid chromatography−mass spectrometry (LCMS) spectra were recorded on Agilent Technologies 6330 Ion Trap instrument. High-resolution electrospray ionization time-of-flight (HR-ESI-TOF) analyses were performed at Scripps Center for Metabolomics and Mass Spectrometry, La Jolla, California. IR spectra were obtained on a Nicolet Nexus 670 FT-IR Instrument using KBr pellets.

Gadolinium concentration was measured by inductively coupled argon plasma (ICP) mass spectrometry (University of Illinois at Urbana−Champaign {UIUC}, Illinois Sustainability Technology Center, Division of the Institute of Natural Resource Sustainability). The sample (0.0500 mL) was added to Optima grade nitric acid (0.500 mL) and heated to 80 °C in a closed vial overnight. The solution was left for 7 weeks before being shipped to UIUC. Samples were also measured by inductively coupled plasma optical emission spectrometry (ICP-OES) (San Diego State University, Ecology Analytical Facility).

X-ray Crystallography. After purification of **4a-NaOTf** and **4b-NaOTf** by chromatography, the compounds were crystallized, and data were acquired and analyzed by the Small Molecule X-ray Crystallography facility at the University of California, San Diego. Compound **4a-NaOTf** was crystallized by slow evaporation of CH$_2$Cl$_2$, whereas **4b-NaOTf** was crystallized by vapor diffusion of diethyl ether into a CH$_2$Cl$_2$ solution at −10 °C.

Synthesis of 9.[59] To a dry 3-neck flask was added triflic anhydride (13.7469 g, 48.7237 mmol, 1.03 equiv relative to (*S*)-methyl lactate) and dry CH$_2$Cl$_2$ (15 mL). An addition funnel was placed on the 3-neck flask and filled with (*S*)-methyl lactate (4.9040 g, 47.1040 mmol), dry *N,N*-diisopropylethylamine (6.3931 g, 49.4631 mmol), and dry CH$_2$Cl$_2$ (5 mL). The contents of the addition funnel were added dropwise under nitrogen to the reaction mixture as the flask was cooled in an ice bath over a period of 10 min before the bath was allowed to warm to room temperature. Reaction completion was monitored by analysis of aliquots by proton and fluorine NMR. The proton NMR showed 2.1% of unreacted alcohol in the reaction mixture. The crude reaction mixture was used directly in the next step without further purification. ^{1}H NMR of an aliquot (CD$_3$OD, 399.8

MHz) showing peaks for **9**: δ 5.25 (q, J = 7.0, 1H), 3.86 (s, 3H), 1.72 (d, J = 7.0, 3H). ^{19}F NMR (CDCl$_3$, 376.1 MHz): δ −75.2 (s) trifluoromethanesulfonate (triflate, TfO) on **9** and −78.4 (s) free triflate ion.

Synthesis of 11. A sample of **8**[60,61] (3.44 g, 15.68 mmol) was taken up in CH$_2$Cl$_2$ (40 mL), and the resulting solution was dried over molecular sieves (beads, grade 512 type 4 Å, 4−8 mesh) overnight. The flask was then chilled in an ice bath under nitrogen. Dry (distilled from CaH$_2$) *N,N*-diisopropylethylamine (12.47 g, 96.48 mmol) was added dropwise, followed by the reaction mixture described above, containing **9** (47.10 mmol assuming 100% yield) via cannula, and the reaction flask was rinsed with CH$_2$Cl$_2$ (3 mL) to complete the transfer of alkylating agent. After 3 h, an aliquot was removed from the supernatant, solvent was removed using a nitrogen stream, and the residue was analyzed in CD$_3$OD by ^{1}H NMR spectroscopy, showing complete disappearance of the formylcyclen signal at 8.12 ppm and the appearance of one major (>92%) singlet at 8.02 ppm. After a total of 4 h of reaction time, the mixture was filtered through a Büchner funnel containing Whatman filter paper (No. 40) to remove molecular sieves, and the solids were rinsed with cold CH$_2$Cl$_2$ (50 mL). The combined CH$_2$Cl$_2$ filtrates were washed with ice water (100 mL). The CH$_2$Cl$_2$ phase was washed with 3% NaOH (3 × 100 mL). The aqueous layers were combined and back-extracted with CH$_2$Cl$_2$ (100 mL). All organic layers were combined and washed with brine (100 mL) and dried over Na$_2$SO$_4$. The mixture was filtered, and the filtrate was concentrated by rotary evaporation, leaving an amber oil (8.21 g) containing intermediate **10** and some **9**. For **10** in the mixture: ^{1}H NMR (CD$_3$OD, 399.8 MHz) δ 8.02 (s, 1H), 4.17 (ddd, J = 5.3, 8.4, 14.0, 1H), 3.89 (ddd, J = 4.2, 9.3, 13.7 1H), 3.678 (s, 3H), 3.671 (s, 6H) [In addition, correlation spectroscopy data suggests additional peaks overlap peaks in this region], 3.585 and 3.583 (two q, each with J = 7.0, total 2H), 3.47 (td, J = 5.2, 14.3 1H), 2.95−2.81 (m, 7H), 2.75 (td, J = 5.1, 14.2, 2H), 2.69−2.62 (m, 3H), 2.50−2.38 (m, 2H), 1.258 (d, J = 7.0, 3H), 1.250 (d, J = 7.2, 3H), 1.215 (d, J = 7.2, 3H). ^{13}C NMR (CD$_3$OD, 100.5 MHz): δ 175.7, 175.6, 175.5, 165.5, 61.2, 60.0, 57.2, 53.8, 51.9, 51.8, 51.7, 51.6, 51.3, 51.1, 51.0, 50.2, 44.0, 15.7, 15.6, 15.2. ^{19}F NMR (CD$_3$OD, 376.1 MHz): δ −80.1 (s). ESI-MS m/z 459.2 (M + H), 481.3 (M + Na), (calculated for M = C$_{21}$H$_{38}$O$_7$N$_4$, 458.27). In addition, minor peaks in the ^{1}H and ^{13}C NMR spectra are present for DOTMA or its Na$^+$ OTf$^−$ adduct, an undesired side-product. There was also evidence of a minor presence of DOTMA by ESI-MS m/z 539.3 (M + Na), (calculated for M = C$_{24}$H$_{44}$O$_8$N$_4$, 516.32). The undesired DOTMA-NaTfO was not removed at this point to minimize the number of purification steps to preserve yield and reduce possible racemization of product

The crude product was dissolved in methanol (100 mL), and the resulting solution was stirred as the flask was chilled in ice. Triflic acid (5.09 g, 33.9 mmol, 2.0 equiv relative to the amount of **8** used; the yield of intermediate **10** was assumed to be 100%) was added over 5 min. After an additional 5 min, the mixture was allowed to warm to room temperature; then it was heated in a 60 °C oil bath for 7 h before being cooled to room temperature and concentrated by rotary evaporation. The residue was stored under vacuum for 10 h, leaving **11** (26.26 g, 33.9 mmol, 100%) as crispy beige foam, which quickly turns sticky on exposure to moisture in air. ^{1}H NMR (CD$_3$OD, 399.8 MHz, digital resolution = 0.20 Hz) δ 5.48 (s, 1H), 4.66 (q, J = 7.2, 1H), 4.37 (q, J = 7.0, 1H), 3.85 (s, 3H), 3.73 (s, 3H), 3.66 (s, 3H), 3.95−3.56 (m, 6H, partially overlapping with other signals and partially hidden quartet at 3.72 ppm), 3.29−3.22 (m, 4H), 3.15−2.95 (m, 6H), 2.84−2.60 (m, 3H), 1.64 (d, J = 7.24, 3H), 1.37 (d, J = 7.1, 3H), 1.36 (d, J = 6.8, 3H). ^{13}C NMR (CD$_3$OD, 100.5 MHz) δ 176.7, 176.5, 171.4, 121.9 (q, J = 318.6), 60.8, 56.5, 56.0, 55.7, 54.1, 53.2, 53.2, 48.8, 48.4, 46.3, 44.6, 44.3, 44.1, 44.0, 42.6. ^{19}F NMR (CD$_3$OD, 376.1 MHz): δ −79.9 (s). ^{23}Na NMR (CD$_3$OD, 376.1 MHz): δ −3.4 (s).

Synthesis of 4b-NaOTf. Triflic anhydride (4.8468 g, 17.2 mmol) was added to a dry 3-neck flask containing dry CH$_2$Cl$_2$ (15 mL). Ester−azide alcohol **12** (2.497 g, 15.7 mmol) and dry ^{i}Pr$_2$NEt (2.2375 g, 17.3 mmol) were added dropwise over 10 min using an addition funnel. The mixture was transparent pale brown. Using a gastight syringe, 90 min after the first Tf$_2$O had been added, a 50 μL aliquot

was removed and quickly added to dry $CDCl_3$ (0.6 mL) in an NMR tube. Analysis by ^{19}F NMR spectroscopy showed singlets at −74.6 and −78.4 ppm for **13** and triflate ion, respectively, and almost no detectable peak at −79.2 (Tf_2O). Analysis by ^1H spectroscopy showed a singlet at 3.89 ppm (CH_3O_2C of product, 3.0 units) and a small singlet at 3.83 (CH_3O_2C of reactant **12**, 0.10 units), indicating that approximately 10% of alcohol **12** remained. An additional portion of Tf_2O (0.5985 g, 2.12 mmol) was added 120 min after the beginning the first Tf_2O addition. Another 6.5 h elapsed before the solution of triflate **13**, which was kept in the freezer, was added to the other reactant solution, prepared as follows: in a separate flask under nitrogen, to salt **11** (26.26 g, derived from 15.68 mmol of formylcyclen **8**) was added CH_2Cl_2 (80 mL) and dry $^iPr_2NEt$ (10.52 g, 81.4 mmol). The flask was chilled in ice, and the solution of triflate ester **13** was added via cannula over 7 min. After an additional 8 min the ice bath was removed, and the mixture was allowed to warm to ambient temperature. After an additional 6 h, using a gastight syringe, a 50 μL aliquot was removed and quickly added to dry $CDCl_3$ (0.6 mL) in an NMR tube. Analysis by ^{19}F NMR spectroscopy showed one major singlet at −80.1 ppm (triflate ion) and a very minor peak at −76.8 (**13**). The flask was chilled in ice, and an ice-cold solution of NaOH (6 g) in water (50 mL) was added. The aqueous phase was extracted with CH_2Cl_2 (2 × 50 mL). The combined CH_2Cl_2 phases were concentrated by rotary evaporation, and the residue was stored under vacuum for 5 h, leaving a brownish solid (10.98 g). Analysis by ^{19}F NMR spectroscopy showed singlets at −76.8 and −80.1 ppm for **13** and product, respectively. The crude product was purified by silica gel flash chromatography (gradient from CH_2Cl_2 to acetonitrile; product elutes with acetonitrile–CH_2Cl_2 0.4:1), affording a beige foamlike solid (total 6.076 g, 8.170 mmol, 52% overall yield from formylcyclen **8**, with 5% DOTMA tetramethyl ester–NaOTf calculated from NMR spectra (not shown)). ^1H NMR (CD_3OD, 399.8 MHz, digital resolution = 0.20 Hz): δ 3.84–3.80 (m, 4H), 3.78 (s, 3H), 3.76 (s, 3H), 3.75 (s, 3H), 3.74 (s, 3H), 3.73–3.67 (m, 2H), 3.65–3.63 (m, 1H), 3.57–3.50 (m, 1H), 3.11–2.07 (m, 4H), 2.75–2.65 (m, 4H), 2.43–2.38 (m, 4H), 2.00–1.91 (m, 2H), 1.26 (d, J = 7.0, 3H), 1.25 (d, J = 7.1, 6H). ^{13}C NMR (CD_3OD, 599.8 MHz): δ 178.4, 178.2, 178.2, 177.4, 59.6, 57.8, 57.8, 57.8, 53.2, 53.1, 53.0, 51.6, 48.5, 46.0, 45.9, 45.9, 45.9, 24.6, 7.83, 7.80. ^{23}Na NMR (CD_3OD, 399.8 MHz): δ 6.6 (br s) and −3.4 (sharper s) in a ratio of 98 to 2, respectively, based on integration of NMR peaks. ^{19}F NMR (CD_3OD, 399.8 MHz): δ −79.9 (s). ESI-LCMS m/z 572.3 (M + H) (calculated for M+ = $C_{25}H_{45}O_8N_7$ = 571.33). Anal. Calcd for $C_{25}H_{45}N_7O_8$ + CF_3NaO_3S (743.73): C, 41.99; H, 6.10; N, 13.18. Found: C, 41.70; H, 5.93; N, 13.58%. IR (KBr): 3442.9 br, 2956.4 s, 2845.7 s, 2099.2 s, 1728.2 s, minor peaks at 2360.4, 1637.5. For examples of Na^+ complexes like **4b-NaOTf**, see refs 62 and 63.

Synthesis of 5a. Methanol (250 mL) was added to a mixture of **4a-NaOTf** (12.96 g, 18.5 mmol) and Pd on carbon (5%, 1.29 g) in a 1 L flask so as to wet the catalyst as quickly as possible. The mixture was stirred as the flask was placed in an ice bath. After 10 min, TfOH (2.868 g, 19.1 mmol) was added over 1 min. The ice bath was removed, and hydrogen was bubbled slowly through the mixture for 9 h. The mixture was stirred for an additional 38 h under static hydrogen atmosphere, hydrogen gas being bubbled through the mixture once for 5 min in the middle of this time period. The mixture was filtered through Celite, and the filter cake was rinsed with methanol (4 × 100 mL). The combined filtrates were concentrated by rotary evaporation, and the syrupy residue was stored under vacuum for 2 weeks, leaving **5a** (15.17 g) as crispy foam, which quickly turns sticky on exposure to moisture in air. The NMR data suggest the presence of two species in CD_3OD solution, likely a mixture of the structure shown (with Na^+ associated with the macrocycle, $δ_{Na}$ = 6.5 ppm) along with free solvated Na^+ ($δ_{Na}$ = −3.4 ppm) and the sodium-free macrocycle. ^1H NMR (CD_3OD, 399.8 MHz): δ 3.81 (s, 3H), 3.79–3.74 (m, 9H), 3.69–3.63 (m, 1H), 3.63–3.40 (m, 4H), 3.27–3.08 (m, 5H), 3.08–2.90 (m, 5H), 2.84–2.57 (m, 4H), 2.48–2.19 (m, 5H), 2.19–1.30 (m, 6H). ^{13}C NMR (CD_3OD, 599.8 MHz): δ 176.6, 176.1, 175.9, 175.1, 174.0, 173.4, 60.5, 56.0, 54.2, 53.9, 52.8, 50.6, 47.0, 45.7, 40.1, 39.3,

29.6, 26.9, 23.2, 19.8. ^{23}Na NMR (CD_3OD, 105.8 MHz): δ 6.5 (br s), −3.4 (s). ^{19}F NMR (CD_3OD, 376.1 MHz): δ −79.7 (s).

Synthesis of 5b (isolated product to be formulated as monohydrate). To a round-bottom flask containing **4b-NaOTf** (7.53 g, contained 7% DOTMA-NaOTf, 10.12 mmol if 100% pure) was added 5% palladium on carbon (0.7530 g) along with MeOH (150 mL) under nitrogen. The mixture was put in an ice bath, and TfOH (1.5781 g, 10.515 mmol) was added over 10 min. Hydrogen gas was bubbled gently through the mixture for 6 h. The vent needle was then removed, and the reaction was kept under hydrogen gas overnight. The mixture was then filtered through a Celite pad into a tared flask. The Celite pad was rinsed with MeOH (2 × 50 mL). The filtrate was concentrated by rotary evaporation and then put under vacuum for 4 d, affording a pale orange syrup (8.85 g, 10.20 mmol, quantitative yield). ^1H NMR (CD_3OD, 599.6 MHz): (δ 3.8–3.6, includes signal from DOTMA) δ 3.80 (s, 3H), 3.75 (s, 3H), 3.74 (s, 6H), 3.67–3.65 (m, 1H), 3.34–3.31 (m, 4H) likely 2H, but obscured by solvent signal, 3.14–3.06 (m, 1H), 3.02 (t of narrow multiplet, J ≈ 14.0, 5H), 2.77 (tdd, J = 13.7, 5.0, 2.7, 2H), 2.69 (tdd, J = 13.7, 6.5, 2.6, 3H), 2.44–2.39 (m, 5H), 2.29–2.20, (m, 4H), 2.09–1.98 (m. 2H), 1.27 (d, J = 7.3, 3H), 1.25 (d, J = 7.0, 8H, 6H from **5b** as well as signal from DOTMA). ^{13}C NMR (CD_3OD, 599.8 MHz): δ 178.4, 178.2, 178.2, 178.1, 176.7, 60.6, 57.7(t), 53.4, 53.0, 48.8, 48.5, 45.9, 40.2, 23.3, 7.8. ^{23}Na NMR (CD_3OD, 105.7 MHz): δ 6.6 (br s), −3.4 (s). ^{19}F NMR (CD_3OD, 376.1 MHz): δ −79.9 (s). Anal. Calcd for $C_{27}H_{48}F_6N_5NaO_{14}S_2$ (867.81): C, 37.37; H, 5.58; N, 8.07. Found: C, 36.71; H, 5.78; N, 7.57%. Calcd for $C_{27}H_{48}F_6N_5NaO_{14}S_2$ + H_2O (885.82): C, 36.61; H, 5.69; N, 7.91.

Model Reaction of DMF with 9. To a dry J. Young resealable NMR tube was added **9** (0.0184 g, 0.07791 mmol, 1.0 equiv) and dry dimethylformamide (DMF) (0.0107 g, 0.14639 mmol, 1.88 equiv), and CD_2Cl_2 was added until the total volume was ∼0.55 mL. The NMR tube was left at room temperature. Proton and fluorine NMR spectra were acquired at different time points (11 min, 1.2 h, 2.2 h, 3.2 h, 6.5 h, 19.7 h, and 7 d) to monitor the evolution and stability of product(s) formed. ^{19}F NMR (CD_2Cl_2, 376.1 MHz): δ −79.1 (s) for the free triflate of the product and −75.7 (s) for the covalently bound triflate of the starting material. As time elapsed the peak at δ −75.7 decreased as a peak at δ −79.1 increased. After 1.3 h, integration of the ^{19}F NMR peaks showed that 77% of the fluorine was in the free triflate ion. After 19.7 h had passed the only ^{19}F NMR peak was the one at δ −79.1 ppm, showing complete consumption of **9**. For the intermediate compound **A** in the reaction mixture: ^1H NMR (CD_2Cl_2, 399.8 MHz): δ 8.93 (s, 1H), 7.96 (s, 1H), 5.55 (q, J = 7.0, 1H), 3.82 (s, 3H), 3.50 (s, 3H), 3.29 (s, 3H), 1.73 (d, J = 7.0, 3H). ^{13}C NMR (CD_2Cl_2, 399.8 MHz): δ 167.9, 160.5, 121.2 (q, J = 320.1, 1C) 81.7, 54.0, 42.6, 37.2, 17.3. ^{19}F NMR (CD_2Cl_2, 399.8 MHz): δ −79.2 (s).

After 22 d, the product formed appears to be stable as seen by the proton NMR spectrum. To test our proposed hydrolysis hypothesis, in the glovebox deoxygenated water (5.5 μL, 0.30 mmol, 1.2 equiv) was added to the reaction mixture in the NMR tube. The reaction was monitored by proton NMR spectroscopy, showing that after 25 min the proton peaks corresponding to **A** were not detectable, and only the peaks for hydrolysis products were seen, indicating that the hydrolysis occurred relatively quickly, which supports the notion that trialkylation of compound **8** to form **10** is accompanied by some overalkylation and loss of the formyl group, leading to the formation of small amounts of DOTMA-NaOTf. For the hydrolysis mixture: ^1H NMR (CD_2Cl_2, 399.8 MHz): δ 8.07 (s, 1H), 5.19 (q, J = 7.0, 1H), 3.72 (s, 3H), 1.49 (d, J = 7.0, 3H); in addition, peaks for residual excess DMF were seen at 7.96 (s, 1H), 2.92 (s, 3H), 2.82 (s, 3H), and a broad peak for water at 4.60 ppm. ^{13}C NMR (CD_2Cl_2, 399.8 MHz): δ 171.1, (163.1, DMF carbonyl carbon), 160.6, 68.6, 52.8, 36.9, 36.0, 31.7, 17.3. ^{19}F NMR (CD_2Cl_2, 399.8 MHz): δ −79.1 (s).

General Method for the Synthesis of Gadolinium and Europium Complexes of N₃-DOTA and N₃-DOTMA Chelates. Complexes **Gd-4a**, **Gd-4b**, **Eu-4a**, and **Eu-4b**. In an open flask, N_3-ester–chelate (**4a** or **4b**, 1.00 mmol, 1.0 equiv) was dissolved in tetrahydrofuran (THF) (15 mL) followed by the addition of water (4 mL). To the above mixture was added $LiOH·H_2O$ (6.0 molar equiv)

while being stirred at 0 °C. The reaction was brought to room temperature, and stirring was continued overnight (16 h). The reaction could be monitored by IR [before addition of LiOH: 2100.5 cm^{-1} (N$_3$), 1733.4 cm^{-1} (C=O); after LiOH: 2092.2 cm^{-1} (N$_3$), 1595.3 cm^{-1} (carboxylate)]. Once complete, the reaction mixture was concentrated by rotary evaporation and stored under oil pump vacuum. The crude hydrolysis product was further used without purification, and the yield was assumed to be 100%; the solid (1.0 equiv from **4a** or **4b** starting material) was dissolved in water (40 mL), and GdCl$_3$·6H$_2$O or EuCl$_3$·6H$_2$O (1.1 molar equiv) was added at room temperature. The pH was adjusted to 7 using 1 M HCl, and the mixture was stirred overnight at 80 °C, under nitrogen. Completion was determined by ESI-MS (direct injection). The solution was then concentrated by freeze-drying, and the residue was dried over phosphorus pentoxide in a desiccator for at least 2 d. Yields could not be calculated because of the uncertain composition of the complexes' counterions (X) as well as other ions accumulated during the synthesis. Even after attempts at purification using ion-exchange columns, elemental analyses tended to give low values, which others have noted for lanthanide-DOTA complexes.[64,65] Since the purification of complexes **Gd-4a**, **Gd-4b**, **Eu-4a**, and **Eu-4b** was not trivial, analogous complexes (**Gd-6a**, **Gd-6b**, **Eu-6a**, and **Eu-6b**) were purified after functionalization with Cbz group.

[Gd(DOTA-N$_3$)]X (**Gd-4a**) was obtained (0.6601 g) from the starting ester−chelate **4a** (0.4516 g, 0.6436 mmol). ^{23}Na NMR (CD$_3$OD, 105.7 MHz): δ −2.10 (br s). ^{19}F NMR (CD$_3$OD, 376.1 MHz): δ −80.11 (s). ^{7}Li NMR (CD$_3$OD, 155.4 MHz): δ −0.39 (br s). ICP-OES (Gd at 342.247 and 335.047 nm); 143.5−145.2 ppm, expected 215.6 ppm (if all material was only Gd-DOTA-N$_3$ anion). HRMS (ESI-TOF) of Gd-DOTA-N$_3$: m/z 651.1130 (M + Na + H), (calculated m/z for (M + Na + H) = (^{12}C)$_{18}$(^{1}H)$_{27}$(^{158}Gd)-(^{14}N)$_7$(^{16}O)$_8$, 651.1138].

[Gd(DOTMA-N$_3$)]X (**Gd-4b**) was obtained (0.7033 g) from the starting ester−chelate **4b** (0.4628 g, 0.6223 mmol). ^{23}Na NMR (CD$_3$OD, 105.7 MHz): δ 0.08 (s). ^{19}F NMR (CD$_3$OD, 376.1 MHz): δ −78.80 (s). ^{7}Li NMR (CD$_3$OD, 155.4 MHz): δ 0.12 (s). ICP-OES(Gd at 342.247 and 335.047 nm); 204.1−207.7 ppm, expected 284.0 ppm (if all material was only Gd-DOTMA-N$_3$ anion. HRMS (ESI-TOF) of Gd-DOTMA-N$_3$: m/z 671.1777 (M + 2H), (calculated m/z for (M + 2H) = (^{12}C)$_{21}$(^{1}H)$_{33}$(^{158}Gd)(^{14}N)$_7$(^{16}O)$_8$, 671.1788).

[Eu(DOTA-N$_3$)]X (**Eu-4a**) was obtained (1.7075 g) was obtained from the starting ester−chelate **4a** (1.0020 g, 1.4281 mmol). ^{23}Na NMR (CD$_3$OD, 105.7 MHz): δ −0.42 (br s). ^{19}F NMR (CD$_3$OD, 376.1 MHz): δ −79.99 (s). ^{7}Li NMR (CD$_3$OD, 155.4 MHz): δ 0.00 (br s). ESI-MS(+): m/2z 318.5 (M + 2Li) (calculated m/z for M = C$_{18}$H$_{27}$EuN$_7$O$_8$, 622.11).

[Eu(DOTMA-N$_3$)]X (**Eu-4b**) (0.5507 g) was obtained from the starting ester−chelate **4b** (0.3478 g, 0.4676 mmol). ^{23}Na NMR (CD$_3$OD, 105.7 MHz): δ 0.15 (s). ^{19}F NMR (CD$_3$OD, 376.1 MHz): δ −78.76 (s). ^{7}Li NMR (CD$_3$OD, 155.4 MHz): δ 0.12 (s). ESI-MS(+): m/z 666.4 (M + 2H); ESI-MS(−): m/z 664.1 (M); (calculated m/z for M = C$_{21}$H$_{33}$GdN$_7$O$_8$, 664.16).

General Method for the Synthesis of Cbz-Protected Esters 6a and 6b. A round-bottom flask was charged with tetraester amine (**5a** or **5b**, 2.4 mmol) and N-(benzyloxycarbonyloxy)succinimide (910 mg, 3.66 mmol), and CH$_2$Cl$_2$ (80 mL) was added. The flask was kept on an ice bath, and the mixture was stirred for 15 min before the addition of triethylamine (1.3 mL, 9.7 mmol). The ice bath was removed, and the reaction mixture was stirred at room temperature overnight. Solvent was removed by rotary-evaporation, and the remaining residue was dissolved in methylene chloride (50 mL) and washed with water (3 × 20 mL). The organic layer was separated, dried over anhydrous sodium sulfate, filtered, and evaporated to give a light yellow gummy mass. The compound was purified using normal phase silica chromatography and a solvent gradient of CH$_2$Cl$_2$ in methanol (from 0 to 80% methanol).

DOTA-Cbz-ester **6a**: (1.24 g, 81%) was obtained from the starting ester−chelate **5a** (1.21 g, 2.4 mmol). ^{1}H NMR (DMSO-d_6, 500 MHz): δ 7.44−7.20 (m, 5H), 5.01 (s, 2H), 3.87−3.44 (m, 16H), 3.37−2.77 (m, 16H), 2.76−2.56 (m, 2H), 2.31−1.82 (m, 3H), 1.80−1.62 (m,

1H), 1.27−1.08 (m, 4H). ESI-MS (+): 638.59 (M + H, 100%) [M = C$_{30}$H$_{47}$N$_5$O$_{10}$, 637.72].

DOTMA-Cbz-ester **6b**: (1.23 g, 74%) was obtained from the starting ester−chelate **5b** (1.34 g, 2.45 mmol). ^{1}H NMR (CDCl$_3$, 500 MHz): δ 7.42−7.23 (m, 5H), 6.50 (s, 1H), 5.09 (s, 2H), 3.77−3.59 (m, 12H), 3.58−3.23 (m, 6H), 3.19−3.01 (m, 2H), 2.99−2.32 (m, 14H), 2.11−1.68 (m, 2H), 1.32−1.11 (m, 9H). ESI-MS (+): 680.31 (M + H, 100%), 546.28 (M−Cbz + H, 55%) [M = C$_{33}$H$_{53}$N$_5$O$_{10}$, 679.4].

General Method for the Synthesis of Gadolinium and Europium Complexes of Cbz-DOTA and Cbz-DOTMA Chelates. Complexes Gd-6a, Gd-6b, Eu-6a, and Eu-6b. In an open flask, Cbz-ester−chelate (**6a** or **6b**, 1.00 mmol) was dissolved in a mixture of THF (6 mL) and MeOH (3 mL) followed by the addition of water (2 mL). An aqueous solution of LiOH·H$_2$O (230 mg in 1 mL of water, 5.45 mmol) was added to the above mixture while being stirred at 0 °C. The reaction was brought to room temperature, and stirring was continued overnight. The mixture was concentrated and redissolved in water (4 mL) followed by adjusting the pH to ∼7 using 0.5 M HCl. Water was removed by freeze-drying, and the remaining solid was checked by ^{1}H NMR spectroscopy to confirm the absence of OMe signals. The crude hydrolysis product was further used without purification; the solid was dissolved in water (20 mL), and a 1 M aqueous solution of GdCl$_3$·6H$_2$O or EuCl$_3$·6H$_2$O (1 mL, 1.00 mmol) was added at room temperature. The pH was adjusted to 7 and maintained by adding a 1.0 M solution of LiOH during the course of the reaction. The mixture was stirred overnight at 65 °C. Solvent was removed by freeze-drying, and the remaining solid was purified over reverse-phase C18 silica using methanol and water (0% to 100%) as eluents. Fractions containing desired compounds were identified by TLC and mass spectral analysis. An aqueous solution of Gd compounds was further passed through a HiTrap SP HP column, which removed lithium ions.

Li[Gd(DOTA-Cbz)] (**Gd-6a**) was obtained (255 mg, 38%) from the starting ester−chelate **6a** (630 mg, 0.91 mmol). ESI-MS(−): 735.26 (M − Li, 100%) (calculated m/z for M = C$_{26}$H$_{35}$GdLiN$_5$O$_{10}$, 742.18].

Li[Gd(DOTMA-Cbz)] (**Gd-6b**) was obtained (313 mg, 47%) from the starting ester−chelate **6b** (580 mg, 0.85 mmol). ESI-MS(−): 777.20 (M − Li, 100%). ESI-MS(+): 791.24 (M + 2Li, 100%) (calculated m/z for M = C$_{29}$H$_{41}$GdLiN$_5$O$_{10}$, 784.23).

Li[Eu(DOTA-Cbz)] (**Eu-6a**) (68 mg, 32% yield) was obtained from the starting ester−chelate **6a** (185 mg, 0.27 mmol). ESI-MS(+): 738.21 (M + H, 100%) (calculated m/z for M = C$_{26}$H$_{35}$EuLiN$_5$O$_{10}$, 737.18).

Li[Eu(DOTMA-Cbz)] (**Eu-6b**) (125 mg, 68% yield) was obtained from the starting ester−chelate **6b** (160 mg, 0.24 mmol). ESI-MS(+): 780.24 (M + H, 74%), 786.15 (M + Li, 100%) (calculated m/z for M = C$_{29}$H$_{42}$EuLiN$_5$O$_{10}$, 779.22).

To create rotationally constrained chelates with increased rotational correlation times, a biotin moiety for avidin binding was added as outlined in Scheme 4.

General Method for the Synthesis of Biotinylated Chelate Esters 7a and 7b. A round-bottom flask was charged with ester−chelate (**5a** or **5b**, 0.15 mmol) and biotinamidohexanoic (LC-biotin) acid NHS-ester (60 mg, 0.13 mmol) followed by the addition of THF (5 mL). The flask was kept on an ice bath, and the mixture was stirred for 15 min before the addition of triethylamine (150 μL, 1.1 mmol). The ice bath was removed, and the reaction mixture was stirred at room temperature for 16 h. The solvent was removed in a rotary evaporator, and the remaining residue was dissolved in CH$_2$Cl$_2$ (20 mL) and washed with water (3 × 5 mL). The organic layer was separated, dried over anhydrous sodium sulfate, filtered, and evaporated to give an off-white solid. The compound was purified using SiO$_2$ and a gradient of CH$_2$Cl$_2$ in methanol (from 0 to 80% methanol).

7a (86 mg, 74%) was obtained from **5a** (78 mg, 0.155 mmol). ^{1}H NMR (CDCl$_3$, 500 MHz): δ 7.29 (t, 1H, J = 5.2 Hz), 6.88 (t, 1H, J = 5.3 Hz), 6.01 (s, 1H), 5.69 (s, 1H), 4.54−4.48 (m, 1H), 4.36−4.29 (m, 1H), 3.81−3.69 (m, 12H), 3.58−3.52 (m, 1H), 3.51−3.34 (m, 3H),

Scheme 4. Synthesis of Biotin–Chelate Conjugates Gd-7a and Gd-7b
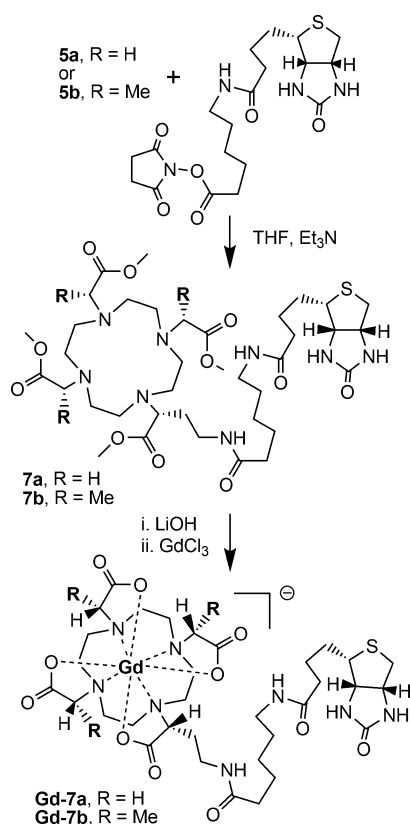
3.24–3.12 (m, 5H), 3.11–2.81 (m, 8H), 2.79–2.70 (m, 1H), 2.65–2.01 (m, 16H), 1.96–1.71 (m, 3H), 1.70–1.28 (m, 11H). ESI-MS(+): 843.60 (M + H, 10%), 865.64 (M + Na, 100%) (calculated m/z for M = $C_{38}H_{66}N_8O_{11}S$, 842.46).

7b (62 mg, 53%) was obtained from **5b** (86 mg, 0.157 mmol). ^{1}H NMR (CDCl$_3$, 500 MHz): δ 7.31 (m, 1H), 6.82 (m, 1H), 5.92 (s, 1H), 5.47 (s, 1H), 4.51 (m, 1H), 4.34 (m, 1H), 3.85–3.61 (m, 15H), 3.55–3.41 (m, 2H), 3.40–3.32 (m, 1H), 3.28–3.11 (m, 4H), 3.01–2.82 (m, 5H), 2.79–2.69 (m, 1H), 2.61–2.44 (m, 4H), 2.44–2.13 (m, 11H), 2.02–1.29 (m, 15H), 1.29–1.13 (m, 9H). ESI-MS(+): 907.68 (M + Na, 100%) (calculated m/z for M = $C_{41}H_{72}N_8O_{11}S$, 884.50).

General Method for the Synthesis of Gadolinium Complexes of Biotin-Chelate Gd-7a and Gd-7b. In an open flask, biotin–tetraester derivative **7a** or **7b** (0.1 mmol) was dissolved in a mixture of THF (2 mL) and MeOH (1 mL) followed by the addition of water (0.5 mL). An aqueous solution of LiOH·H$_2$O (21.5 mg in 0.5 mL water, 0.5 mmol) was added to the above mixture while being stirred at 0 °C. The reaction was brought to room temperature, and stirring was continued overnight. The mixture was concentrated and redissolved in water (4 mL) followed by adjusting the pH to ~7 using 0.5 M HCl. Water was completely removed by freeze-drying, and the remaining solid was checked by ^{1}H NMR spectroscopy to confirm the absence of OMe signals. The crude hydrolysis product was further used without purification; the solid was dissolved in water (5 mL), and a 1 M aqueous solution of GdCl$_3$ (115 μL, 0.12 mmol) was added at room temperature. The pH was adjusted to 7 and maintained by adding a 1.0 M solution of LiOH during the course of the reaction. The mixture was stirred for 40 h at 55 °C. The solvent was removed by freeze-drying, and the remaining solid was purified over reverse-phase C18 silica using methanol and water (0% to 100%) as eluents. Fractions containing desired salts **Gd-7a** or **Gd-7b** were identified by TLC and mass spectral analysis. Aqueous solutions of Gd salts were further passed through a HiTrap SP HP column.

Gd-7a (40 mg, 42% yield) was obtained from the starting ester–chelate **7a** (86 mg, 0.1 mmol). ESI-MS(−): 940.30 (M-Li, 100%). ESI-

MS(+): 942.10 (M − Li + 2H, 100%) [M = $C_{34}H_{54}Gd_1Li_1N_8O_{11}S_1$, 946.30]. ESI-HRMS(−): 942.4705 (M − Li + 2H, 96%), 964.4579 (M − Li + H + Na, 100%) (calculated m/z for M = $C_{34}H_{54}Gd_1Li_1N_8O_{11}S_1$, 947.3034).

Gd-7b (37 mg, 53% yield) was obtained from the starting ester–chelate **7b** (62 mg, 0.07 mmol). ESI-MS(−): 982.3 (M − Li, 100%). ESI-MS(+): 984.3 (M − Li + 2H, 100%) [calculated m/z for M = $C_{37}H_{60}Gd_1Li_1N_8O_{11}S_1$, 989.35). ESI-HRMS(+): 990.3564 (M + H, 100%) (calculated m/z for M = $C_{37}H_{60}Gd_1Li_1N_8O_{11}S_1$, 989.3503).

Oxygen-17 NMR Measurements. NMR measurements of ^{17}O were performed as described by Laurent et al.[66] Solutions of **Gd-6a** and **Gd-6b** were prepared in distilled water (pH 6.5–7.0) at concentrations of 23 mM. Solutions (0.35 mL) were transferred to 5 mm o.d. NMR tubes, and ^{17}O NMR measurements were made at 11.7 T in a Bruker AVANCE-500 spectrometer (Bruker, Karsruhe, Germany). The temperature was regulated by air or nitrogen flow controlled by a Bruker BVT 3200 unit. ^{17}O transverse relaxation times of distilled water (pH = 6.5–7) were measured using a Carr–Purcell Meiboom–Gill (CPMG) sequence and a subsequent two-parameter fit of the data points. The 90° and 180° pulse lengths were 27.5 and 55 μs, respectively. The ^{17}O T_2 values of water in the solutions of complexes were obtained from line width measurements. All spectra were proton decoupled. Data are presented as the reduced transverse relaxation rate $(1/T_2^R = 55.55/(q \times [\text{complex}] \times 1/T_2^P))$, where [complex] is the molar concentration of the complex, q is the number of inner sphere coordinated water molecules, and $1/T_2^P$ is the paramagnetic transverse relaxation rate. Data analysis and treatment was performed as described by Vander Elst et al.,[67] Muller et al.,[68] and Laurent et al.[69]

Proton Nuclear Magnetic Relaxation Dispersion (NMRD) Measurements. Proton NMRD measurements were made over a magnetic field range of 0.47 mT to 1.0 T on a Stelar Spin fast field cycling (FFC) NMR relaxometer (Stelar, Mede (PV), Italy). Three different solutions of each complex were prepared in 50 mM N-(2-hydroxyethyl)piperazine-N′-ethanesulfonic acid (HEPES) buffer, pH = 7.35, with 150 mM NaCl. Measurements were performed on 0.800 mL samples in 10 mm o.d. NMR tubes. Additional relaxation rates were measured at 20 and 60 MHz on a Bruker Minispec mq-20 and mq-60 at temperatures specified in Figure 4 and matching temperatures used for all samples.

Biotin–Avidin Complexation. Three separate sample concentrations of **7a** and **7b** were prepared with avidin. In separated tubes a solution of 50 mM HEPES, pH = 7.35, with 150 mM NaCl was added to six tubes containing avidin for final concentrations of 0.22 mM. Chelates were added such that [chelate]/[avidin] never exceeded 3.2 (i.e., the ratio was always less than 4 to prevent saturation of avidin) at concentrations of 0.553, 0.692, and 0.700 mM Gd(III) for **7a** and 0.267, 0.315, and 0.448 mM Gd(III) for **7b**.

■ **RESULTS**

The progress of trialkylation of **8** (Scheme 1) was followed by analysis of aliquots by ^{1}H NMR spectroscopy, looking for disappearance of the formyl resonance for **8**, as well as any peaks other than those for the intermediate **9**. Subsequent deprotection of the N-formyl group required only 2 equiv of acid in methanol, giving compound **11** as a triflate salt in quantitative yield.

Subsequent alkylation of the triflate salt of **11** in situ using freshly prepared **13** led to isolation of **4b-NaOTf** after column chromatography using CH$_2$Cl$_2$–CH$_3$CN. The structure of **4b-NaOTf** as a NaOTf adduct was strongly suggested by clearly visible peaks in both ^{23}Na and ^{19}F NMR spectra, and was ultimately verified by X-ray crystallography (see Discussion below). Careful analysis of bulk samples of the product revealed a second, minor (<10%) component, ultimately identified as the NaOTf adduct of the tetramethyl ester of DOTMA, which must have arisen at some stage from loss of the N-formyl group of **8** or **9**.
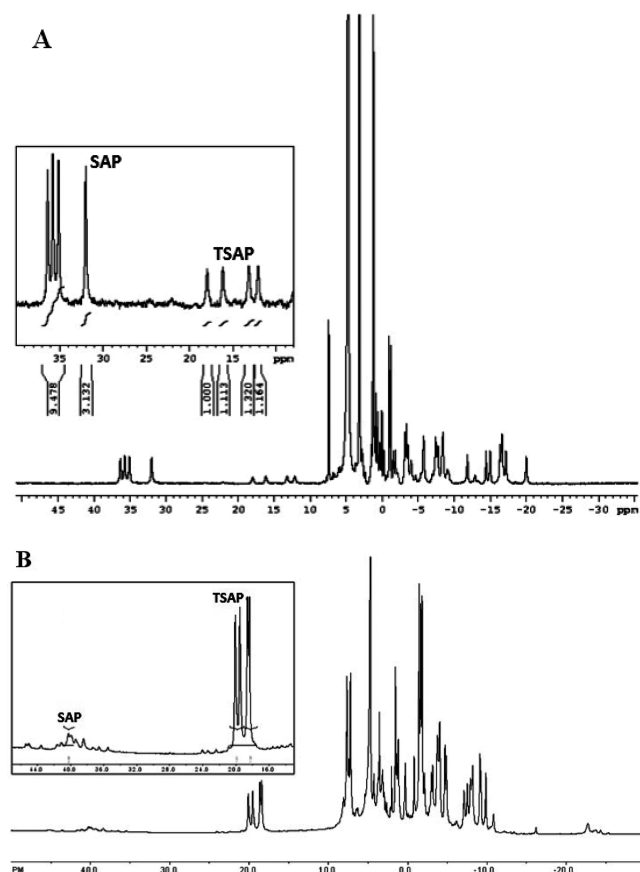
A

B

Figure 2. Proton NMR of Eu-Cbz chelates showing the SAP/TSAP ratio. (top) **Eu-6a**; (bottom) **Eu-6b**.
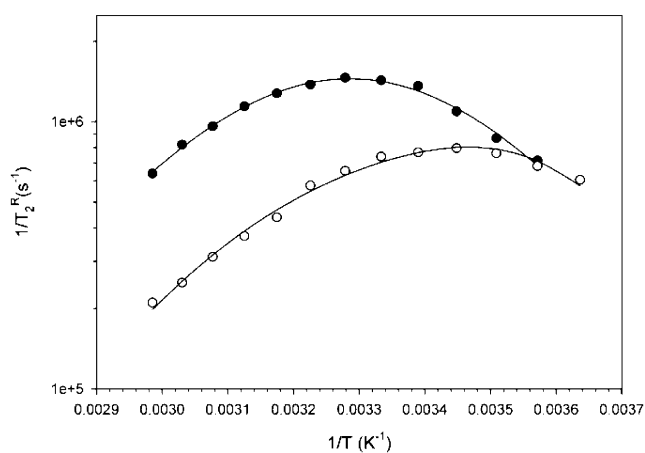

Figure 3. ^{17}O NMR measurement of the reduced transverse relaxation time as a function of the reciprocal of the temperature: **Gd-6a** (●) and **Gd-6b** (○).

The point at which the formyl protecting group was lost is strongly suggested by results of a model reaction using DMF (Scheme 2). Compound **9** and dry DMF were combined in CD_2Cl_2 under dry conditions in a resealable NMR tube, allowing for in situ monitoring of reaction progress without having to disturb the reaction by removing aliquots. With a half-life of about 1 h, a stable intermediate formed (compound **A**) as evidenced by proton and fluorine NMR spectral data. The methine proton on the chiral carbon appeared at 5.55 ppm, the formyl proton appeared at 8.93 ppm, and a fluorine
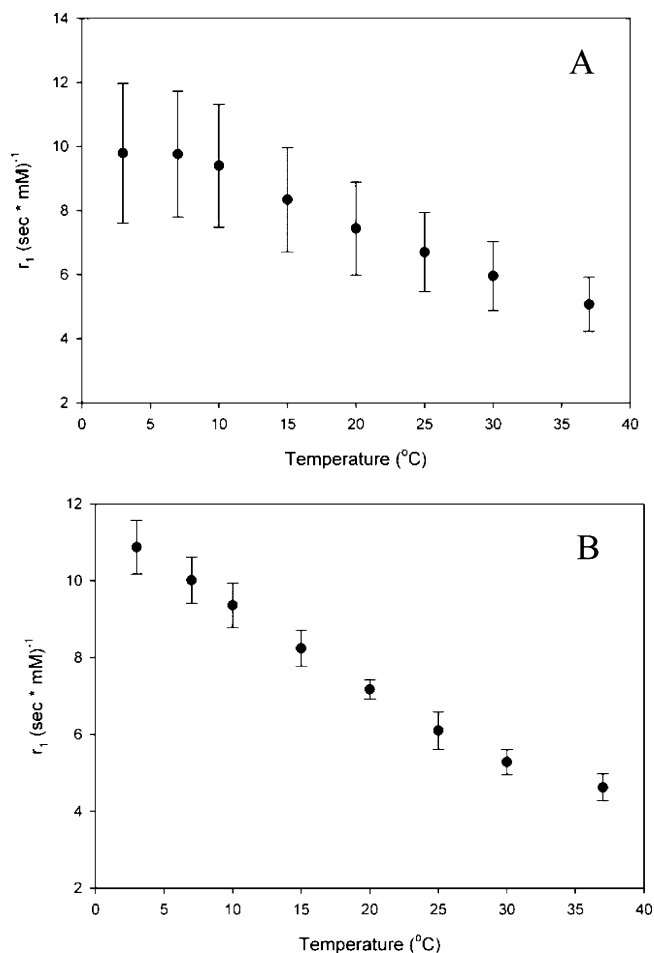

Figure 4. Variable-temperature relaxometry at 0.47 T showing dependence of relaxivity on temperature. (A) **Gd-6a**; (B) **Gd-6b**. Standard errors were determined using three samples.

peak for free triflate ion appeared at −79.1 ppm. Upon addition of water, **A** quickly hydrolyzed to **B**, as shown by proton and fluorine NMR data. The proton on the chiral carbon shifted upfield to 5.19 ppm and the formyl proton shifted upfield to 8.07 ppm, whereas in ^{19}F NMR spectra the free triflate ion signal remained at −79.1 ppm.

Below we discuss the X-ray crystal structure of **4b-NaOTf**. Samples of **4b-NaOTf** containing 5 to 10% of DOTMA impurity were used in subsequent experiments, where the presence of the impurity did not interfere with conjugation because it lacks a reactive side chain group.

Subsequent hydrogenation of the azide (Scheme 1) proceeded smoothly in the presence of one added equivalent of TfOH, without which the amine formed during hydrogenation attacked the ester of the unique side chain, resulting in an unwanted lactam. The resulting triflate salts of the amine derivative **5b-NaOTf** was neutralized by Et_3N and acylated by an external reagent (e.g., in Schemes 3 and 4, biotinamidohexanoic acid of Cbz NHS esters, forming **6a**, **6b**, **7a**, or **7b**). Subsequent basic hydrolysis using LiOH and water−THF mixtures, followed by complexation with Gd(III) or Eu(III) at slightly acidic pH, delivered chelates for further study.

The difference in the water residence times on Gd(III) complexes of DOTA and DOTMA result from the differences in the relative populations of conformational isomers, denoted square antiprismatic (SAP) and twisted square antiprismatic

Table 1. Parameters Obtained by the Theoretical Analysis of the ^{17}O NMR Experimental Data

	τ_M^{310} (ns)	τ_V^{298} (ps)	$\Delta H^{\ddagger}$ (kJ mol^{-1})	$B \times 10^{20}$ (s^{-2})	E_V (kJ mol^{-1})	$A/\hbar \times 10^6$ (rad s^{-1})	$\Delta S^{\ddagger}$ (J mol^{-1} K^{-1})
Gd-6a	100.8 ± 4.7	4.86 ± 0.56	54.1 ± 0.52	1.99 ± 0.229	0.102 ± 19	−2.95 ± 0.203	63.3 ± 2.2
Gd-6b	41.6 ± 5.2	5.23 ± 0.40	63.1 ± 0.198	6.37 ± 0.493	8.12 ± 3.98	−3.0 ± 0.146	99.7 ± 0.407

(TSAP). The TSAP isomer exchanges more quickly. Alpha substitution of the acetate arms attached to the four nitrogens on DOTA creates DOTMA, featuring four chiral centers, and favors the TSAP isomer with the homochiral diastereomer (either the *R,R,R,R* or the *S,S,S,S* enantiomer) having the highest TSAP/SAP ratio.[54,56,57] Woods et al.[57] used ^{1}H NMR spectroscopy of Eu(III) complexes to differentiate the various diastereomers and determine the relative ratio of TSAP/SAP in each case. We therefore used proton NMR of Eu(III) complexes of Cbz derivatives **Eu-6a** and **Eu-6b**, Figure 2. The **Eu-6b** has a much higher TSAP/SAP ratio (Figure 2B) than that of **Eu-6a** (Figure 2A). Moreover, the fact that only two sets of peaks are seen demonstrates that the use of base to deprotect the methyl esters did not significantly epimerize the chiral centers, which would have resulted in up to 16 stereoisomers and a large number of peaks in the axial region (downfield of 15 ppm). Moreover, the high TSAP/SAP ratio for **Eu-6b** demonstrates that the conformational properties of the macrocycle or its complexes are not detectably altered by inclusion of unique side chain of novel derivative **6b**. Woods et al.[57] assumed that the conformational behavior of Eu(III) and Gd(III) complexes would be the same in their analysis, and we use the same reasonable assumption. This implies that the bifunctional Gd(III)-DOTMA derivatives should have shorter water residence times than their Gd(III)-DOTA analogues.

To confirm the proton NMR data and calculate the actual water residence time, we used ^{17}O NMR to measure the reduced transverse relaxation rate of the water molecules in the inner coordination sphere of the complexes as a function of temperature (see Figure 3).

Analysis of the results at 37 °C showed that the new DOTA analogue **Gd-6a** had a longer water residence time than the new DOTMA analogue **Gd-6b**, 100.8 versus 41.6 ns, respectively (Table 1). Decreasing the temperature increases the rotational correlation time and the water residence time, which have opposite effects on the relaxivity. For rapidly rotating complexes, whose relaxivity is not limited by long water residence times, decreasing the temperature with the subsequent increase in rotational correlation time will increase the relaxivity. If the water residence time limits the relaxivity, decreasing the temperature will decrease the relaxivity. We used variable-temperature relaxometry to analyze the temperature dependence of the relaxivity of **Gd-6a** and **Gd-6b**, Figure 4. At 37 °C the relaxivities of the two chelates are approximately equal, which is expected for similar Gd(III) systems with one inner sphere water molecule whose rotational correlation time dominates the relaxivity. Decreasing the temperature results in an increase in relaxivity for both chelates until about 10 °C. When the relaxivity for the **Gd-6a** levels off (Figure 4A), the relaxivity of **Gd-6b** continues to increase (Figure 4B), which is expected on the basis of the τ_M data in Table 1. In the case of **Gd-6b**, where the data benefit from smaller error bars, the value at 2.5 °C is clearly greater than the value at 10 °C and at all other higher temperatures.

The results for the Cbz derivatives **Gd-6a** and **Gd-6b** suggest that the relaxivity of rotationally constrained analogues of **6a** with an ethylamino linker are limited by the water residence

time and that rotationally constrained compounds made from the DOTMA analogue **6b** should have higher relaxivities. To test this hypothesis, we prepared the biotinylated version of the two chelates (**Gd-7a** and **Gd-7b**) and used the avidin−biotin complexation (ABC) reaction to increase the rotational correlation time or rotationally constrain the two compounds. The small-molecule biotin analogues **Gd-7a** and **Gd-7b** are rapidly rotating and have the same relaxivities and similar NMRD profiles, Figure 5. Adding avidin results in the binding
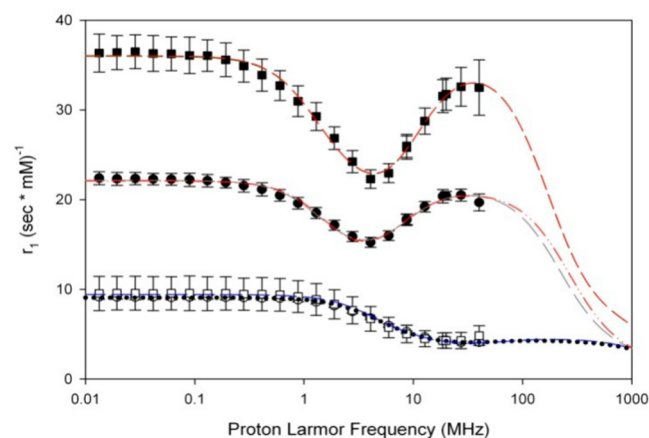

Figure 5. NMRD profiles of **Gd-7a** (circles) and **Gd-7b** (squares) with (filled) and without (open) avidin at 37 °C, showing the effects of biotin−avidin binding on relaxivity.

of biotin and increases the rotational correlation time and relaxivity. The Cbz derivatives **6a** and **6b** were studied to provide preliminary data for the further investigation of derivatives **7a** and **7b**.

NMRD profiles of the long chain (LC) biotinylated Gd chelates in the presence of avidin show a peak in the high-field region characteristic of slowly rotating complexes.[41] In the presence of avidin, **Gd-7b** has higher relaxivities than **Gd-7a** at all corresponding magnetic field strengths, consistent with a shorter water residence time on the new DOTMA derivative **Gd-7b**.

The variable-temperature relaxometry results, coupled with the calculated water residence times of the Cbz derivatives **Gd-6a** and **Gd-6b**, and the NMRD profiles of biotinylated derivatives **Gd-7a** and **Gd-7b** predict that the relaxivity of the rotationally constrained **Gd-7a + avidin** might be limited by the water residence time, while that of the **Gd-7b + avidin** might be dominated by the rotational correlation time. To test this hypothesis, we performed variable-temperature relaxometry on the avidin complexed derivatives (Figure 6). Decreasing the temperature has no effect on the relaxivity of the **Gd-7a + avidin**, whereas the relaxivity of **Gd-7b + avidin** monotonically increases with decreasing temperature.

■ DISCUSSION

Synthesis. As evidenced mainly by NMR, X-ray crystallography, and mass spectroscopy, we prepared four new bifunctional chelates (**4a-**, **4b-**, **5a-**, and **5b-NaOTf**) and
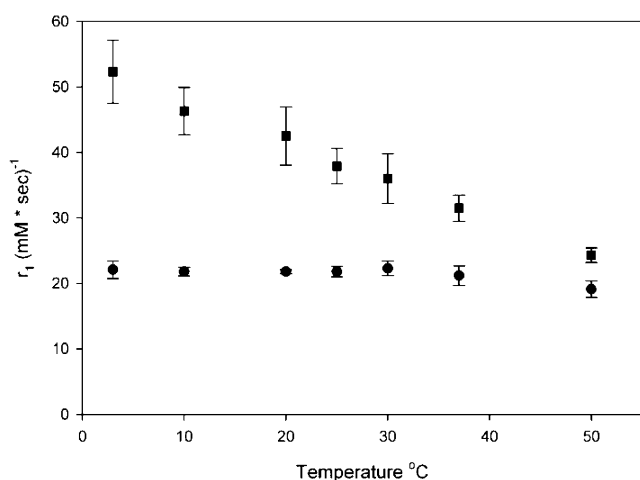
Figure 6. Variable-temperature relaxometry of **Gd-7a** (filled circles) and **Gd-7b** (filled squares) with avidin at 0.47 T. Note that for a given temperature, each **Gd-7b** value is significantly different from the **Gd-7a** value at $P < 0.001$. Among **Gd-7a** values, the 50 °C value is significantly different ($P \leq 0.001$) from all others, and the 3 °C value is significantly different ($P \leq 0.001$) than all others except the 10 °C value. Other groups of values significantly different ($P \leq 0.001$): 37 °C and 3, 10, 20 °C; 30 °C and 3 and 10 °C; 25 °C and 3 and 10 °C.

successfully complexed them to Gd to make novel contrast agents. Two different functional groups (N_3, **4** and NH_2, **5**) of each chelate (DOTA, **a**; DOTMA, **b**) are designed for coupling to either alkynes using click chemistry or carboxylic acids using standard peptide coupling chemistry.

The syntheses of **4a**- and **4b-NaOTf** were designed to minimize the role of chromatographic purifications, and they make exclusive use of triflate as a counterion for several reasons. Previous work had shown that the leaving group from **9** could be displaced in an S_N2 fashion with high fidelity, and because of relatively rapid reaction rates with amine nucleophiles, subsequent epimerization of the newly formed chiral center was minimized.[59] None of the other leaving groups used (other sulfonates, halides) gave satisfactory results. The work also showed that although **9** could be isolated and even distilled, such treatment tended to lower the enantiomeric purity of both **9** and its alkylation products.[59] Thus, here both triflate electrophiles **9** and **13** were made fresh and used as mixtures, rather than being isolated or stored.

N-formylcyclen (**8**) was an attractive monoprotected cyclen derivative,[70] readily made according to literature procedures, which are reported to give the monohydrate.[60,61] Previously, in our hands the trialkylation of **8** with the primary halide $BrCH_2CO_2{}^tBu$ and subsequent N-deprotection proceeded without incident,[71] whereas here, after similar treatment of **8** with **9**, because some tetraalkylated side product was formed, evidence was gathered that the *N*-formyl group was being lost during alkylation. The control experiment shown in Scheme 2 shows how incomplete drying of the alkylation reaction might lead to formyl group loss: DMF was quickly alkylated, and the resulting iminium ion suffered rapid hydrolysis. We hypothesized that the water in the hydrated form of **8** and/or wet methanol helped facilitate partial premature loss of the *N*-formyl group and allowed a fourth alkylation event, leading to formation of DOTMA tetramethyl ester–NaOTf adduct. Indeed, drying the formylcyclen–CH_2Cl_2 solution with molecular sieves prior to alkylation reduced the amount of

side product to levels below 10%, though we could not avoid its formation entirely. Formamide alkylations are known (for examples, see refs 72 and 73), and subsequent hydrolyses are also known.[74−76]

Turning to the deprotection of **10**, though HCl could be used, the presence of chloride counterion turned out to interfere with the subsequent alkylation by **13**, because of chloride displacement of the triflate. In theory, one could neutralize the HCl salt and isolate the free amine for alkylation, but in practice, we found that higher overall yields could be obtained by the procedure shown, with triflic acid.

Using NMR, elemental analysis, and X-ray crystallography, it was found that the azide analogues had a sodium cation coordinated to macrocycle as well as a triflate counterion. These ions were present even after purification by liquid chromatography and crystallization. There are similar macrocycles[62,63,77−84] that contain a sodium ion bound in place by ring nitrogens and carbonyl-containing arms. The average bond distances between Na−O and Na−N of **4a-NaOTf** were 2.540(8) Å and 2.556(7) Å, respectively. And the average bond distances between Na−O and Na−N of **4b-NaOTf** (Figure 7) were 2.502(7) Å and 2.562(7) Å, respectively.
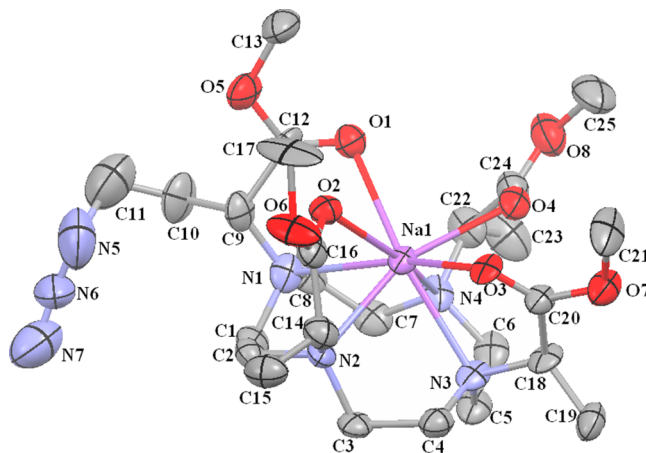

Figure 7. Thermal ellipsoid plot of **4b-NaOTf** drawn at 35% probability level. Hydrogen atoms and triflate counterion were omitted for clarity.

These bond distances fall reasonably within the average range of distances found for similar crystal structures (CCDC search results: Na−O: 2.513(30) Å and Na−N: 2.622(7) Å). An interesting trend found in the crystal structure of **4b-NaOTf**, among the four molecules that form the unit cell, was the Na−N bond was longest for the nitrogen with the azide moiety; this could be due to steric effects. In contrast, only one of the two molecules in the unit cell of **4a-NaOTf** had a significantly longer Na−O and Na−N distance (2.823(11) Å and 2.642(11) Å, respectively) on the nitrogen and oxygen that are part of the azide moiety. The crystallographic data obtained of **4a-NaOTf** and **4b-NaOTf** show that the azide moiety does not significantly alter the conformation of macrocycle, for example by disrupting chelation by the ester oxygens or ring nitrogens.

The proton NMR spectrum of **Eu-6b** (Figure 2B) is consistent with an *R,R,R,R* configuration for the compound, given the broken symmetry caused by the unique amino butyric acid arm, which causes four unique m_{ax} peaks to be seen between δ 18 and 20 ppm. Similarly, four m_{ax} peaks were seen for the *R,R,R,S* isomer of Eu(III)-DOTMA where the *R*-

configured center breaks the symmetry.[57] Our NMR data for **Eu-6b** convincingly show the presence of *either* the *R,R,R,R* or *S,S,S,S* stereoisomer, but by themselves do not discriminate between these two possibilities; what does discriminate between the possible stereoisomers is the synthetic starting materials and known S_N2 inversion. Our synthesis of **5b** and derivatives was designed to produce the *R,R,R,R* enantiomer. The crystal structure of intermediate **4b-NaOTf** verifies its *R,R,R,R* configuration, and for **4a-NaOTf**, the single stereocenter was in the *R* configuration. However, the one caveat is that the assignments are rigorously proven only for the single crystals analyzed. In the case of **4b-NaOTf**, analysis of bulk sample (50−100 mg) was accomplished by ^{13}C NMR spectroscopy, with particular attention paid to the carbonyl region (178.5 to 178.0 ppm). Other than a minor peak for DOTMA-NaOTf at 178.1 ppm, only four singlets were seen, at 178.3, 178.2, 178.2, and 177.4 ppm. We conclude that no other diastereomers were present in greater than 3% concentration. If another diastereomer were present, unless all of its carbonyl peaks were overlapping with those seen, we estimate that the limit of detection was 3%.

We note the landmark 1992 paper[85] of Renn and Meares with title "Large Scale Synthesis" of a bifunctional DOTA analogue in quantities of "up to 10 g" in a linear nine-step synthesis with overall yield 5.6%. Several steps required reverse-phase HPLC purifications. We thank a reviewer for pointing out that the Meares work accomplished synthetically challenging cyclen ring substitution in the form of a *para*-nitrobenzyl group. Subsequent insightful papers from the groups of Sherry and Woods[86] report synthesis of the corresponding *para*-nitrobenzyl DOTMA analogue and a series of significant studies of the structure and dynamics of their lanthanide complexes, but somewhat surprisingly, our search of the literature found no reported use of the bifunctional nature of these DOTMA derivatives to date. In contrast, here we report synthesis of arm-substituted bifunctional DOTMA analogues on similar ca. 10 g scale but in only five steps from cyclen to the azide derivative **4b-NaOTf** in about 40% overall yield, with only one chromatography step. Moreover, of equal or greater significance, as highlighted below, we show that the proposal that a macromolecular DOTMA agent should have higher relaxivity than its DOTA counterpart is correct, thanks to our ability to conjugate the new DOTMA derivative in such a way as to leave the coordination sphere intact.

Relaxivity Properties. Dunand et al.[56] demonstrated that "the water-exchange rate is definitely independent of the solution structure for both the SAP and TSAP isomers, and, hence, the overall water exchange only depends on the SAP/TSAP isomeric ratio." The proton NMR of **Eu-6a** and **Eu-6b** clearly shows the SAP/TSAP ratio is much greater for **Eu-6a** relative to **Eu-6b**. The water residence time for the **Gd-6a** at 37 °C is approximately 2.5 times longer than that of **Gd-6b** (101 vs 42 ns), which is consistent with the larger SAP/TSAP ratio.

The difference in water residence times of the Gd(III)-Cbz chelate complexes coupled with the small molecular size imply that the relaxivities at 25 and 37 °C should be similar, but following an increase in the rotational correlation times, the values of relaxivity should differ. Therefore, we increased the rotational correlation time by decreasing the temperature. If the relaxivity of a chelate was limited by the rotational correlation time, then decreasing the temperature will increase the relaxivity. Decreasing the temperature also has the effect of increasing the water residence time. If the relaxivity of a chelate

were limited by the water residence time, then decreasing the temperature would decrease the relaxivity. Figure 4 shows a variable-temperature relaxometry experiment on the **Gd-6a** and **Gd-6b**. Both chelates exhibit increasing relaxivities as the temperature is decreased from 37 to 15 °C. However, from 15 to 3 °C the relaxivity of the **Gd-6a** levels off, while that of **Gd-6b** continues to increase. The relaxivity of **Gd-6a** levels off because the increase in relaxivity associated with increasing the rotational correlation time is now offset by the decrease in relaxivity associated with increasing the water residence time. In contrast, the water residence time of **Gd-6b** at 37 °C is lower than that of **Gd-6a**, but even by lowering the temperature to 3 °C, it has not yet reached a value that offsets changes in the relaxivity associated with increasing the rotational correlation time.

The shorter water residence time and the variable-temperature relaxometry indicate that the rotationally constrained Gd(III)-DOTMA derivative should have a higher relaxivity than a similarly constrained Gd(III)-DOTA derivative. Rotationally constraining low molecular weight Gd(III) chelates increases the rotational correlation time. One can rotationally constrain the chelates by increasing the viscosity[55] or attaching the Gd(III) chelate to a macromolecule either covalently or noncovalently.[40,41,45] We elected to increase the rotational correlation time of the two types of chelates by noncovalently attaching them to avidin through the ABC reaction. ABC was first done for a derivative of Gd(III)-diethylenetriaminepentaacetate (Gd(III)-DTPA) by Langereis et al.[87] and later by Geninatti Crich et al.[88] Biotin binds to avidin and streptavidin with an extremely high noncovalent binding constant. Each protein has four biotin binding sites. Prior to the addition of avidin to the biotinylated chelates, the NMRD profiles are found to be the same with the characteristic features of rapidly rotating molecules. This is expected as the rotational correlation time dominates the relaxivity for small Gd(III) chelates with these water residence times. Adding avidin increases the rotational correlation time and significantly increases the relaxivity of both biotinylated chelates, with the relaxivity of **Gd-7b** increasing more than that of **Gd-7a**. The NMRD profiles of **Gd-7a + avidin** and **Gd-7b + avidin** also exhibit the characteristic peak of the relaxivity in the high-field region. The higher relaxivity across all magnetic field strengths for **Gd-7b** relative to **Gd-7a** are consistent with the well-accepted view that the water residence time limits the relaxivity of constrained Gd(III)-DTPA and Gd(III)-DOTA chelate systems.

We used the long-chain (LC) derivative of biotin that consists of biotin plus an aminohexanoic acid chain. This longer chain helps guarantee unimpeded access of the biotin conjugate to the avidin binding site, meaning the affinity of the biotin conjugate would be equal to that of biotin itself, but also has the potential for additional rotational freedom about the long chain linking the chelate to the protein. There is the possibility for a shorter overall rotational correlation time resulting from segmental motions. We therefore used variable-temperature relaxometry to determine if further increases in the rotational correlation time increased the relaxivity. The relaxivity at 20 MHz of the **Gd-7a** with avidin (**Gd-7a + avidin**) was constant while decreasing the temperature from 50 to 3 °C, whereas the relaxivity of **Gd-7b** (**Gd-7b + avidin**) almost doubled (see Figure 6). A one-way repeated-measures analysis of variance gave $P \leq 0.001$ and a power of the test with α equal to 0.050:1.000. We used the Holm−Sidak method for a pairwise

multiple comparison to isolate the groups that differ from one another. In the presence of avidin the relaxivities of **Gd-7b** at all temperatures, except 50 °C, significantly differed from the relaxivities at all temperatures of **Gd-7a** with $P \leq 0.001$. In the presence of avidin the relaxivity of **Gd-7b** at 50 °C was not significantly different from the relaxivities of **Gd-7a** at 3, 10, 20, 25, 30, 37, and 50 °C. In the presence of avidin none of the relaxivities of the **Gd-7a** were significantly different at any temperature from itself in the presence of avidin. The relaxivities of **Gd-7b** in the presence of avidin at all temperatures differed significantly, $P \leq 0.001$, except the relaxivities at 3 and 10; 10 and 20; 20 and 25; 20 and 30; 25 and 30; 25 and 37; 30 and 37 °C.

The implication from the foregoing data that the water residence time limits the relaxivity of rotationally constrained DOTA complexes (e.g., **Gd-7a** + **avidin**) is consistent with other reports. We have shown that the water residence time of a generation 6 ammonia core polyamidoamine dendrimer with an isothiocyanatobenzyl-DOTA derivative, having the linker attached to a ring carbon, limits the relaxivity.[48] Increasing the temperature from 5 to 35 °C results in an increase in the relaxivity from 25 to 32 $(s \times mM)^{-1}$. The increase in relaxivity associated with decreasing the water residence time (that results from increasing the temperature) offsets and exceeds the decrease in relaxivity associated with decreasing the rotational correlation time (that results from increasing the temperature). The water residence time dominates when the relaxivity increases with increasing temperature. Using the same chelate attached to ethylenediamine core polyamidoamine dendrimers Bryant et al.[89] reported that the relaxivity levels off at around generation 7. The relaxivities at 23 °C and 20 MHz for the generations 5, 7, 9, and 10 are 30, 35, 36, and 36 $(s \times mM)^{-1}$, respectively. These values are consistent with the 32 $(s \times mM)^{-1}$ obtained for the generation 6 ammonia core, reported by us.[48] Tweedle's results are also consistent with the relaxivities reported for dendrimers.[55] His group used viscous solutions to reduce the rotational correlation time and obtained maximum relaxivity values of 35 $(s \times mM)^{-1}$ for rotationally constrained Gd(III)-DOTA systems. The experimentally obtained values match closely to the theoretical values calculated with Solomon−Bloembergen−Morgan theory using experimental values for the water residence time, which predicted the water residence time limits the relaxivity of rotationally constrained Gd(III)-DOTA systems. While our results demonstrate that the relaxivity of the Gd(III)-DOTA derivative **Gd-7a** is limited by the water residence time, the maximum relaxivity observed for **Gd-7a** + **avidin** is substantially lower 22 $(s \times mM)^{-1}$ (see Table 2) than that reported for other systems[89] [30 to 36 $(s \times mM)^{-1}$]. It is possible that the lower relaxivity results from a longer water residence time caused by the association of the chelate with avidin. However, the **Gd-7a** + **avidin** relaxivity is similar to that of other biotin−avidin systems (see Table 2).

Avidin is a highly glycosylated protein, and the −OH groups may act like those on poly(ethylene glycol) to reduce the relaxivity.[90] Note that fitting the NMRD profile while letting the water residence time float, instead of fixing it at the value for the Cbz-Gd(III)-DOTA measured by ^{17}O NMR, yields a value for the water residence time that is quite long relative to that measured for our DOTA derivative **Gd-6a** (408 vs 101 ns, respectively). This is about 10 times the value calculated for **Gd-7b** + **avidin** (45 ns) by letting the water residence time float during the NMRD fitting process. Both fitting methods

Table 2. Comparison of Relaxivities (r_1) of Selected Compounds Similar to Those in This Work

compound	r_1 (mM^{-1} s^{-1})	tesla	temp (°C)	ref.
Gd(III)-DTPA	4.2	0.47	35	46
Gd(III)-DOTA	3.4	0.47	37	91
Gd(III)-DOTMA	4.2	0.47	40	92
G = 5 PAMAM (Gd-DOTA)	30	0.59	35	48
G = 6 PAMAM (Gd-DOTA)	31	0.59	35	48
G = 7 PAMAM (Gd-DOTA)	34	0.59	25	48
G =10 PAMAM (Gd-DOTA)	36	0.47	23	48
biotinylated Gd-DTPA	6.1 ± 0.2	1.5	20	46
(biotinylated) **Gd-7a**	8.7	0.47	37	this work
(biotinylated) **Gd-7b**	8.7	0.47	37	this work
avidin−biotinylated GdL1/Av (DOTA)	18.1	0.47	25	93
avidin−biotinylated GdL2/Av (DOTA)	17.4	0.47	25	93
avidin−biotinylated Gd-DTPA	17.5 ± 0.3	1.5	20	46
avidin−biotinylated **Gd-7a**	22	0.47	20	this work
avidin−biotinylated **Gd-7b**	45	0.47	20	this work

are reasonable, and therefore we cannot disregard the results of using either model: letting the water residence time float or fixing it to values measured by ^{17}O NMR.

While letting the water residence time float gives similar rotational correlation times, using fixed water residence times gives us different rotational correlation times. We cannot eliminate the second possibility, because such a change in rotational correlation time could result from protein−chelate associations.[94,95] The constant relaxivity observed for **Gd-7a** with avidin in the variable-temperature NMRD data of Figure 5 supports an increase in the water residence time to longer values on binding to avidin. One would expect a decrease in the relaxivity associated with a decrease in temperature as was observed with a generation 6 ammonia core PAMAM dendrimer coated with a Gd(III)-DOTA surface.[48] The inability to differentiate between changes in rotational correlation time or changes in the water residence time associated with the binding of the chelate to avidin highlight the main problem with multiparameter NMRD profile fits: *there is no unique solution, and often multiple solutions have similar quality of fits.* At best the parameter values obtained are estimates and suffer from a lack of accuracy. Large errors can result in the values of the parameters because the fits start with assigning a value for the distance between the water proton and metal ion. Usually values for proton−metal distances are obtained from X-ray crystallographic data,[96] and it is well-known from protein studies that solution structures and crystal structures can differ significantly. In the case of the water proton−metal distances a small error in the proton−metal distance can cause significantly larger errors in the five fitted parameters because of the inverse sixth power relationship $1/r^6$ of the water proton−metal distance. In short, while the quantitative accuracy of the fits are always subject to question, qualitative conclusions can be made from NMRD profile fits especially when comparing similar chelates.

The relaxivity of **Gd-7b** in the presence of avidin [32 ± 2 (s × mM)$^{-1}$ at 37 °C] is lower than that reported for highly constrained derivatives, such as the 58 (s × mM)$^{-1}$ value obtained by Tweedle[55] for DOTMA in viscous solution. However, our own results at a lower temperature of 3 °C [52 ± 5 (s × mM)$^{-1}$] show the effects of increased rotational correlation time. The lower relaxivity of **Gd-7b + avidin** at 37 °C may be the result of segmental motions associated with using the long-chain version of biotin. Using biotin itself, without the hexanoic acid spacer, should result in higher relaxivities. The fact that observed relaxivity for the rotationally constrained **Gd-7b** is consistent with those reported in the literature, whereas that of the Gd(III)-LC-DOTA, **Gd-7a**, derivative is much lower may result from steric effects of the CH$_3$ groups on the ligand arms. The CH$_3$ groups on the ligand arms of **Gd-7b** may interfere with any interactions that were hypothesized, to prolong the water residence time or reduce the number of inner-sphere water molecules, to occur between **Gd-7a** and avidin.

The four novel bifunctional chelates (**4a-**, **4b-**, **5a-**, and **5b-NaOTf**) are readily accessible for further studies of their lanthanide complexes. The bifunctional octadentate chelate design enables Gd(III) to be coordinated while maintaining respectable contrast properties and accessibility for more chemistry at the azide/amine moiety. Measurements show that the constrained derivative of **Gd-7b** has a higher relaxivity than that of constrained derivative of **Gd-7a** due to a larger TSAP/SAP ratio; moreover, the relaxivity of **Gd-7b** is dominated by rotational correlation time, unlike **Gd-7a**, which is influenced more by water residence time.

CONCLUSIONS

We reported a concise and efficient synthesis of new bifunctional chelates, notably those containing four stereogenic centers derived from the chiral pool. Using Gd and Eu complexation, the conformations and MRI relevant properties were determined. One significant finding is that for the novel bifunctional materials, comparing the DOTA- and DOTMA-derived chelates, the Gd(III)-DOTMA core has a shorter water residence time; when rotationally constrained, the core has as much as 40% higher relaxivity at 37 °C than the constrained conventional Gd(III)-DOTA chelates. The higher relaxivity has the potential to increase the sensitivity of molecular imaging or reduce the dose of targeted agents. The two other chelates with an azide functionality, N$_3$-DOTA (deprotected **4a**) and N$_3$-DOTMA (deprotected **4b**), are suitable to use with click chemistry for future coupling possibilities to target molecules.[58] In summary, we show that a macromolecular DOTMA agent has higher relaxivity than its DOTA counterpart, thanks in part to the ability to covalently attach the new DOTMA derivatives without altering the coordination sphere and water exchange rates. The new bifunctional compounds are expected to be versatile because of the ability to attach the optimal DOTMA-type chelate using either azide or amine functionality, without disturbing favorable relaxivity properties.

ASSOCIATED CONTENT

Ⓢ Supporting Information

CIF files for **4a-** and **4b-NaOTf**, an ORTEP diagram for **4a-NaOTf**, ESI-TOF of **Gd-4a** and **Gd-4b**, and the NMRD fitting data. This material is available free of charge via the Internet at http://pubs.acs.org.

AUTHOR INFORMATION

Corresponding Author

*E-mail: dbgrotjahn@mail.sdsu.edu.

Notes

The authors declare no competing financial interest.

ACKNOWLEDGMENTS

REFERENCES

(1) Tofts, P. S.; Brix, G.; Buckley, D. L.; Evelhoch, J. L.; Henderson, E.; Knopp, M. V.; Larsson, H. B.; Lee, T. Y.; Mayr, N. A.; Parker, G. J.; Port, R. E.; Taylor, J.; Weisskoff, R. M. *J. Magn. Reson. Imaging* **1999**, *10*, 223−232.

(2) Huang, W.; Li, X.; Morris, E. A.; Tudorica, L. A.; Seshan, V. E.; Rooney, W. D.; Tagge, I.; Wang, Y.; Xu, J.; Springer, C. S., Jr. *Proc. Natl. Acad. Sci. U.S.A.* **2008**, *105*, 17943−17948.

(3) Keunen, O.; Johansson, M.; Oudin, A.; Sanzey, M.; Rahim, S. A.; Fack, F.; Thorsen, F.; Taxt, T.; Bartos, M.; Jirik, R.; Miletic, H.; Wang, J.; Stieber, D.; Stuhr, L.; Moen, I.; Rygh, C. B.; Bjerkvig, R.; Niclou, S. P. *Proc. Natl. Acad. Sci. U.S.A.* **2011**, *108*, 3749−3754.

(4) de Groot, J. F.; Lamborn, K. R.; Chang, S. M.; Gilbert, M. R.; Cloughesy, T. F.; Aldape, K.; Yao, J.; Jackson, E. F.; Lieberman, F.; Robins, H. I.; Mehta, M. P.; Lassman, A. B.; Deangelis, L. M.; Yung, W. K. A.; Chen, A.; Prados, M. D.; Wen, P. Y. *J. Clin. Oncol.* **2011**, *29*, 2689−2695.

(5) Gallez, B.; Lacour, V.; Demeure, R.; Debuyst, R.; Dejehet, F.; De Keyser, J. L.; Dumont, P. *Magn. Reson. Imaging* **1994**, *12*, 61−69.

(6) Josephson, L.; Groman, E. V.; Menz, E.; Lewis, J. M.; Bengele, H. *Mag. Res. Imaging* **1990**, *8*, 637−646.

(7) Konda, S. D.; Aref, M.; Brechbiel, M.; Wiener, E. C. *Invest. Radiol.* **2000**, *35*, 50−57.

(8) Reimer, P.; Weissleder, R.; Lee, A. S.; Buettner, S.; Wittenberg, J.; Brady, T. J. *Radiology* **1991**, *178*, 769−774.

(9) Schaffer, B. K.; Linker, C.; Papisov, M.; Tsai, E.; Nossiff, N.; Shibata, J.; Bogdanov, A., Jr.; Brady, T. J.; Weissleder, R. *Magn. Reson. Imaging* **1993**, *11*, 411−417.

(10) Sipkins, D. A.; Cheresh, D. A.; Kazemi, M. R.; Nevin, L. M.; Bednarski, M. D.; Li, K. C. *Nat. Med. (N.Y., NY, U.S.)* **1998**, *4*, 623−626.

(11) Vera, D. R.; Buonocore, M. H.; Wisner, E. R.; Katzberg, R. W.; Stadalnik, R. C. *Acad. Radiol.* **1995**, *2*, 497−506.

(12) Bulte, J. W. M.; Douglas, T.; Witwer, B.; Zhang, S. C.; Strable, E.; Lewis, B. K.; Zywicke, H.; Miller, B.; van Gelderen, P.; Moskowitz, B. M.; Duncan, I. D.; Frank, J. A. *Nat. Biotechnol.* **2001**, *19*, 1141−1147.

(13) Hinds, K. A.; Hill, J. M.; Shapiro, E. M.; Laukkanen, M. O.; Silva, A. C.; Combs, C. A.; Varney, T. R.; Balaban, R. S.; Koretsky, A. P.; Dunbar, C. E. *Blood* **2003**, *102*, 867−872.

(14) Kraitchman, D. L.; Heldman, A. W.; Atalar, E.; Amado, L. C.; Martin, B. J.; Pittenger, M. F.; Hare, J. M.; Bulte, J. W. M. *Circulation* **2003**, *107*, 2290−2293.

(15) Modo, M.; Cash, D.; Mellodew, K.; Williams, S. C. R.; Fraser, S. E.; Meade, T. J.; Price, J.; Hodges, H. *NeuroImage* **2002**, *17*, 803−811.

(16) Bulte, J. W. M. *AJR, Am. J. Roentgenol.* **2009**, *193*, 314−325.

(17) Lauffer, R. B.; Greif, W. L.; Stark, D. D.; Vincent, A. C.; Saini, S.; Wedeen, V. J.; Brady, T. J. *J. Comput. Assist. Tomogr.* **1985**, *9*, 431−438.

(18) Lauffer, R. B.; Vincent, A. C.; Padmanabhan, S.; Villringer, A.; Saini, S.; Elmaleh, D. R.; Brady, T. *J. Magn. Reson. Med.* **1987**, *4*, 582−590.

(19) Geninatti Crich, S.; Cabella, C.; Barge, A.; Belfiore, S.; Ghirelli, C.; Lattuada, L.; Lanzardo, S.; Mortillaro, A.; Tei, L.; Visigalli, M.; Forni, G.; Aime, S. *J. Med. Chem.* **2006**, *49*, 4926−4936.

(20) Stefania, R.; Tei, L.; Barge, A.; Geninatti Crich, S.; Szabo, I.; Cabella, C.; Cravotto, G.; Aime, S. *Chem.—Eur. J.* **2009**, *15*, 76−85.

(21) Beloueche-Babari, M.; Chung, Y. L.; Al-Saffar, N. M. S.; Falck-Miniotis, M.; Leach, M. O. *Br. J. Cancer* **2010**, *102*, 1−7.

(22) Remy, C.; Von Kienlin, M.; Lotito, S.; Francois, A.; Benabid, A. L.; Decorps, M. *Magn. Reson. Med.* **1989**, *9*, 395−401.

(23) Weiner, M. W.; Hetherington, H.; Hubesch, B.; Karczmar, G.; Massie, B.; Maudsley, A.; Meyerhoff, D. J.; Sappey-Marinier, D.; Schaefer, S.; Twieg, D. B.; Matson, G. B. *NMR Biomed.* **1989**, *2*, 290−297.

(24) Al-Saffar, N. M. S.; Jackson, L. E.; Raynaud, F. I.; Clarke, P. A.; Ramirez de Molina, A.; Lacal, J. C.; Workman, P.; Leach, M. O. *Cancer Res.* **2010**, *70*, 5507−5517.

(25) Glunde, K.; Bhujwalla, Z. M. *Semin. Oncol.* **2011**, *38*, 26−41.

(26) Koul, D.; Shen, R.; Kim, Y.-W.; Kondo, Y.; Lu, Y.; Bankson, J.; Ronen, S. M.; Kirkpatrick, D. L.; Powis, G.; Yung, W. K. A. *Neuro-Oncol.* **2010**, *12*, 559−569.

(27) Ouwerkerk, R. *Methods Mol. Biol.* **2011**, *711*, 175−201.

(28) Perman, W. H.; Turski, P. A.; Houston, L. W.; Glover, G. H.; Hayes, C. E. *Radiology* **1986**, *160*, 811−820.

(29) Boada, F. E.; Tanase, C.; Davis, D.; Walter, K.; Torres-Trejo, A.; Couce, M.; Hamilton, R.; Kondziolka, D.; Bartynski, W.; Lieberman, F. *Conf. Proc. IEEE Eng. Med. Biol. Soc.* **2004**, *7*, 5238−5241.

(30) Kwong, K. K.; Belliveau, J. W.; Chesler, D. A.; Goldberg, I. E.; Weisskoff, R. M.; Poncelet, B. P.; Kennedy, D. N.; Hoppel, B. E.; Cohen, M. S.; Turner, R.; Cheng, H.-m.; Brady, T. J.; Rosen, B. R. *Proc. Natl. Acad. Sci. U.S.A.* **1992**, *89*, 5675−5679.

(31) Menon, R. S.; Ogawa, S.; Kim, S. G.; Ellermann, J. M.; Merkle, H.; Tank, D. W.; Ugurbil, K. *Invest. Radiol.* **1992**, *27* (Suppl 2), S47−S53.

(32) Ogawa, S.; Lee, T. M.; Kay, A. R.; Tank, D. W. *Proc. Natl. Acad. Sci. U.S.A.* **1990**, *87*, 9868−9872.

(33) Ogawa, S.; Lee, T. M.; Nayak, A. S.; Glynn, P. *Magn. Reson. Med.* **1990**, *14*, 68−78.

(34) Manabe, Y.; Longley, C.; Furmanski, P. *Biochim. Biophys. Acta* **1986**, *883*, 460−467.

(35) Shreve, P.; Aisen, A. M. *Magn. Reson. Med.* **1986**, *3*, 336−340.

(36) Wiener, E.; Tomalia, D.; Lauterbur, P. C. *Proc. Soc. Magn. Reson. Med.* **1990**, 1106.

(37) Wiener, E. C.; Brechbiel, M. W.; Brothers, H.; Magin, R. L.; Gansow, O. A.; Tomalia, D. A.; Lauterbur, P. C. *Magn. Reson. Med.* **1994**, *31*, 1−8.

(38) Burton, D. R.; Forsen, S.; Franek, F.; Novotny, J. *FEBS Lett.* **1979**, *102*, 249−252.

(39) Caravan, P.; Ellison, J. J.; McMurry, T. J.; Lauffer, R. B. *Chem. Rev. (Washington, DC, U.S.)* **1999**, *99*, 2293−2352.

(40) Koenig, S. H.; Brown, R. D., 3rd *Magn. Reson. Med.* **1984**, *1*, 478−495.

(41) Lauffer, R. B. *Chem. Rev. (Washington, D. C.)* **1987**, *87*, 901−927.

(42) Jacques, V.; Dumas, S.; Sun, W. C.; Troughton, J. S.; Greenfield, M. T.; Caravan, P. *Invest. Radiol.* **2010**, *45*, 613−624.

(43) Freed, J. *J. Chem. Phys.* **1978**, *68*, 4034−4037.

(44) Koenig, S. H.; Kellar, K. E. *Magn. Reson. Med.* **1995**, *34*, 227−233.

(45) Lauffer, R. B.; Brady, T. J.; Brown, R. D., 3rd; Baglin, C.; Koenig, S. H. *Magn. Reson. Med.* **1986**, *3*, 541−548.

(46) Aime, S.; Botta, M.; Fasano; Paoletti; S.; Anelli, P. L.; Uggeri, F.; Virtuani, M. *Inorg. Chem.* **1994**, *33*, 4707−4711.

(47) González, G.; Powell, D. H.; Tissières, V.; Merbach, A. *J. Phys. Chem.* **1994**, *98*, 53−59.

(48) Wiener, E.; Narayanan, V. *Adv. Dendritic Macromol.* **2002**, *5*, 129−247.

(49) Micskei, K.; Helm, L.; Brucher, E.; Merbach, A. *Inorg. Chem.* **1993**, *32*, 3844−3850.

(50) Aime, S.; Gianolio, E.; Longo, D.; Pagliarin, R.; Lovazzano, C.; Sisti, M. *ChemBioChem* **2005**, *6*, 818−820.

(51) Schuehle, D. T.; Polasek, M.; Lukes, I.; Chauvin, T.; Tóth, É.; Schatz, J.; Hanefeld, U.; Stuart, M. C. A.; Peters, J. A. *Dalton Trans.* **2010**, *39*, 185−191.

(52) Tei, L.; Gugliotta, G.; Baranyai, Z.; Botta, M. *Dalton Trans.* **2009**, *44*, 9712−9714.

(53) Dumas, S.; Jacques, V.; Sun, W.-C.; Troughton, J. S.; Welch, J. T.; Chasse, J. M.; Schmitt-Wilich, H.; Caravan, P. *Invest. Radiol.* **2010**, *45*, 600−612.

(54) Brittain, H.; Desreux, J. *Inorg. Chem.* **1984**, *23*, 4459−4466.

(55) Shukla, R. B.; Kumar, K.; Weber, R.; Zhang, X.; Tweedle, M. *Acta Radiol., Suppl.* **1997**, *412*, 121−123.

(56) Dunand, F. A.; Dickins, R. S.; Parker, D.; Merbach, A. E. *Chem.—Eur. J.* **2001**, *7*, 5160−5167.

(57) Aime, S.; Botta, M.; Garda, Z.; Kucera, B. E.; Tircso, G.; Young, V. G.; Woods, M. *Inorg. Chem.* **2011**, *50*, 7955−7965.

(58) Mastarone, D. J.; Harrison, V. S. R.; Eckermann, A. L.; Parigi, G.; Luchinat, C.; Meade, T. J. *J. Am. Chem. Soc.* **2011**, *133*, 5329−5337.

(59) Effenberger, F.; Burkard, U.; Willfahrt, J. *Liebigs Ann. Chem.* **1986**, 314−333.

(60) Dischino, D. D.; Delaney, E. J.; Emswiler, J. E.; Gaughan, G. T.; Prasad, J. S.; Srivastava, S. K.; Tweedle, M. F. *Inorg. Chem.* **1991**, *30*, 1265−1269.

(61) Platzek, J.; Blaszkiewicz, P.; Gries, H.; Luger, P.; Michl, G.; Müller-Fahrnow, A.; Radüchel, B.; Sülzle, D. *Inorg. Chem.* **1997**, *36*, 6086−6093.

(62) Moore, D. A. PCT Int. Appl. WO2007106546 A2, 2007.

(63) Xu, J.; Sun, G.; Rossin, R.; Hagooly, A.; Li, Z.; Fukukawa, K.-i.; Messmore, B. W.; Moore, D. A.; Welch, M. J.; Hawker, C. J.; Wooley, K. L. *Macromolecules (Washington, DC, U.S.)* **2007**, *40*, 2971−2973.

(64) Faulkner, S.; Pope, S. J. A. *J. Am. Chem. Soc.* **2003**, *125*, 10526−10527.

(65) Pershagen, E.; Nordholm, J.; Borbas, K. E. *J. Am. Chem. Soc.* **2012**, *134*, 9832−9835.

(66) Laurent, S.; Vander Elst, L.; Muller, R. *Contrast Media Mol. Imaging* **2006**, *1*, 128−137.

(67) Vander Elst, L.; Maton, F.; Laurent, S.; Seghi, F.; Chapelle, F.; Muller, R. N. *Magn. Reson. Med.* **1997**, *38*, 604−614.

(68) Muller, R.; Raduchel, B.; Laurent, S.; Platzek, J.; Pierart, C.; Mareski, P.; Vander Elst, L. *Eur. J. Inorg. Chem.* **1999**, 1949−1955.

(69) Laurent, S.; Vander Elst, L.; Houze, S.; Guerit, N.; Muller, R. N. *Helv. Chim. Acta* **2000**, *83*, 394−406.

(70) Suchy, M.; Hudson, R. H. E. *Eur. J. Org. Chem.* **2008**, 4847−4865.

(71) Huang, Z.; Sengar, R. S.; Nigam, A.; Abadjian, M.-C.; Potter, D. M.; Grotjahn, D. B.; Wiener, E. C. *Invest. Radiol.* **2010**, *45*, 641−654.

(72) Hafner, K.; Vöpel, K. H.; Ploss, G.; König, C. *Org. Synth., Coll. Vol.* **1973**, *5*, 431−433.

(73) Abramson, S.; Berkovich-Berger, D.; Dagan, S.; Goldberg, I.; Golender, L.; Grabarnik, M. N.; Lemcoff, G.; Weinman, S.; Fuchs, B. *Eur. J. Org. Chem.* **2007**, *12*, 1957−1975.

(74) Feenstra, R. W.; Stokkingreef, E. H. M.; Nivard, R. J. F.; Ottenheijm, H. C. J. *Tetrahedron* **1988**, *44*, 5583−5595.

(75) Knorr, R.; Löw, P.; Hassel, P.; Bronberger, H. *J. Org. Chem.* **1984**, *49*, 1288−1290.

(76) Alder, R. W.; Blake, M. E.; Bufali, S.; Butts, C. P.; Orpen, A. G.; Schütz, J.; Williams, S. J. *J. Chem. Soc., Perkin Trans. 1* **2001**, 1586−1593.

(77) Tsukube, H.; Mizutani, Y.; Shinoda, S.; Okazaki, T.; Tadokoro, M.; Hori, K. *Inorg. Chem.* **1999**, *38*, 3506−3512.

(78) Kumar, K.; Chang, C. A.; Francesconi, L. C.; Dischino, D. D.; Malley, M. F.; Gougoutas, J. Z.; Tweedle, M. F. *Inorg. Chem.* **1994**, *33*, 3567−3575.

6567

dx.doi.org/10.1021/ic500085g | *Inorg. Chem.* 2014, 53, 6554−6568

(79) Dickins, R. S.; Howard, J. A. K.; Moloney, J. M.; Parker, D.; Peacock, R. D.; Siligardi, G. *Chem. Commun. (Cambridge, U.K.)* **1997**, 1747−1748.

(80) Dickens, R. S.; Howard, J. A. K.; Maupin, C. L.; Moloney, J. M.; Parker, D.; Peacock, R. D.; Riehl, J. P.; Siligardi, G. *New J. Chem.* **1998**, 22, 891−899.

(81) Shinoda, S.; Nishimura, T.; Tadokoro, M.; Tsukube, H. *J. Org. Chem.* **2001**, 66, 6104−6108.

(82) Govenlock, L. J.; Howard, J. A. K.; Moloney, J. M.; Parker, D.; Peacock, R. D.; Siligardi, G. *J. Chem. Soc., Perkin Trans. 2* **1999**, 2415−2418.

(83) Gunnlaugsson, T.; Brougham, D. F.; Fanning, A.-M.; Nieuwenhuyzen, M.; O'Brien, J. E.; Romain, V. *Org. Lett.* **2004**, 6, 4805−4808.

(84) Tsukube, H.; Mizutani, Y.; Shinoda, S.; Tadokoro, M.; Hori, K. *Tetrahedron Lett.* **1997**, 38, 5021−5024.

(85) Renn, O.; Meares, C. F. *Bioconjugate Chem.* **1992**, 3, 563−569.

(86) Woods, M.; Kovacs, Z.; Zhang, S.; Sherry, A. D. *Angew. Chem., Int. Ed.* **2003**, 42, 5889−5892. Woods, M.; Botta, M.; Avedano, S.; Wang, J.; Sherry, A. D. *Dalton Trans.* **2005**, 3829−3837. Tircso, G.; Webber, B. C.; Kucera, B. E.; Young, V. G.; Woods, M. *Inorg. Chem.* **2011**, 50, 7966−7979. Webber, B.; Woods, M. *Inorg. Chem.* **2012**, 51, 8576−8582.

(87) Langereis, S.; Kooistra, H.-A. T.; van Genderen, M. H.; Meijer, E. W. *Org. Biomol. Chem.* **2004**, 2, 1271−1273.

(88) Geninatti Crich, S.; Barge, A.; Battistini, E.; Cabella, C.; Coluccia, S.; Longo, D.; Mainero, V.; Tarone, G.; Aime, S. *J. Biol. Inorg. Chem.* **2005**, 10, 78−86.

(89) Bryant, L. H., Jr.; Brechbiel, M. W.; Wu, C.; Bulte, J. W.; Herynek, V.; Frank, J. A. *J. Magn. Reson. Imaging* **1999**, 9, 348−352.

(90) Manjappa, A. S.; Chaudhari, K. R.; Venkataraju, M. P. *J. Controlled Release* **2011**, 150, 2−22. Hermanson, G. *Bioconjugate Techniques,* 2nd ed.; Academic Press: London, U.K., 2008.

(91) Meyer, D.; Schaefer, M.; Doucet, D. *Invest. Radiol. (Suppl. 1)* **1992**, 25, S53−S55.

(92) Ranganathan, R. S.; Raju, N.; Fan, H.; Zhang, X.; Tweedle, M. F.; Desreux, J. F.; Jacques, V. *Inorg. Chem.* **2002**, 41, 6856−6866.

(93) Tei, L.; Barge, A.; Geninatti Crich, S.; Pagliarin, R.; Negri, V.; Ramella, D.; Cravotto, G.; Aime, S. *Chem.—Eur. J.* **2010**, 16, 8080−8087.

(94) Aime, S.; Barge, A.; Botta, M.; Terreno, E. *Met. Ions Biol. Syst.* **2003**, 40, 643−682.

(95) Aime, S.; Gianolio, E.; Terreno, E.; Giovenzana, G. B.; Pagliarin, R.; Sisti, M.; Palmisano, G.; Botta, M.; Lowe, M. P.; Parker, D. *J. Biol. Inorg. Chem.* **2000**, 5, 488−497.

(96) Avedano, S.; Botta, M.; Haigh, J. S.; Longo, D. L.; Woods, M. *Inorg. Chem.* **2013**, 52, 8436−8450.